

# 7

## Anatomy, Physiology, and Function of Auditory End-Organs in the Frog Inner Ear

DWAYNE D. SIMMONS, SEBASTIAAN W.F. MEENDERINK,  
AND PANTELIS N. VASSILAKIS

### 1. Overview

The vertebrate ear is a highly sensitive frequency analyzer that receives sound through a specialized accessory apparatus (the external and middle ears) prior to its transmission to discrete end-organs containing sensory hair cells (the inner ear). Although there are significant differences in the structures used to receive and analyze sound, amphibian and mammalian ears function very similarly to each other. With few exceptions, the amphibian ear consists of a middle ear and an inner ear, but no external ear. As schematized in Figure 7.1, the amphibian middle ear has an exposed eardrum (tympanic membrane) overlying a funnel-shaped tympanic cavity that connects to the inner ear near the base of the skull (see Mason, Chapter 6, for a review of the amphibian middle ear). The amphibian inner ear or otic labyrinth is unique among vertebrate animals in that it has two sensory organs specialized for the reception of airborne sound, the amphibian papilla (AP) and the basilar papilla (BP). These sensory papillae reside within the posterior portion of the otic labyrinth and are contained in ventrally located recesses of the large, fluid-filled saccular chamber shared with two vibration-sensitive macular organs, the sacculus and lagena (Fig. 7.1). Both the AP and BP chambers have a thin contact membrane that separates periotic perilymph from the endolymph fluid of the saccular chamber.

Sound energy captured by the eardrum as well as other areas along the body of a frog is converted into fluid displacements and travels along pathways of the otic labyrinth that lead into the endolymphatic spaces of the inner ear (Hetherington et al. 1986; Lewis and Lombard 1988; Purgue and Narins 2000a). The sound path eventually leads into the AP and BP recesses before exiting into the caudal portion of the periotic canal and the round window (Purgue and Narins 2000a). Similar to the mammalian ear, the amphibian ear demonstrates exquisite intensity sensitivity and sharp frequency selectivity that are likely to arise from nonlinear, active amplification processes.

How theories of mammalian auditory function apply to amphibian hearing is not known. Mechanisms of tuning and sensitivity have been extensively studied in the mammalian cochlea. It is generally agreed that the initial stage of inner ear

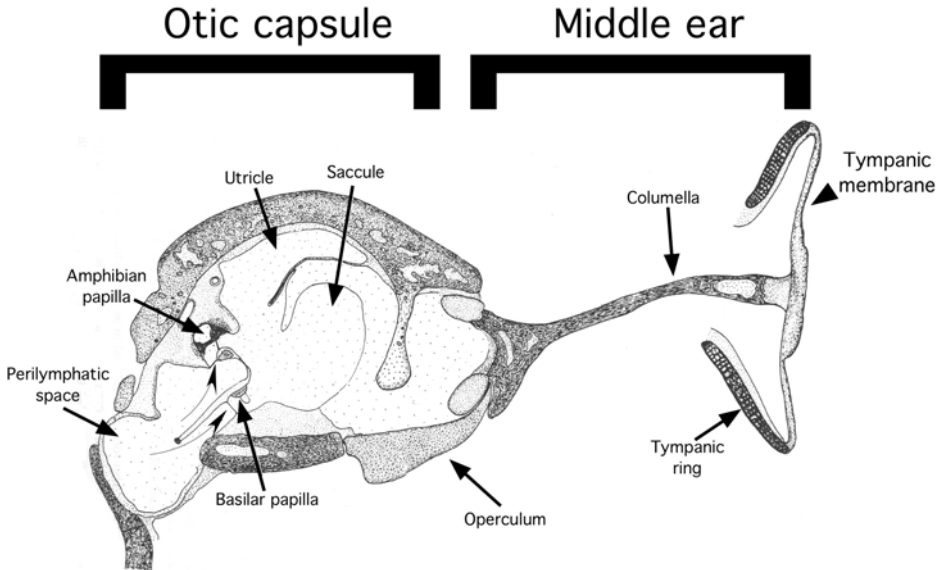


FIGURE 7.1. A schematic representation of the frog's ear. Modified from Wever, Ernest Glen; *the Amphibian Ear*. © 1985 Princeton University Press. Reprinted by permission of Princeton University Press.

frequency selectivity is achieved through the specialized mechanical properties of the basilar membrane, giving rise to a traveling wave (Von Békésy 1960; West 1985). Such traveling waves may be enhanced by electrically driven somatic movements of specialized outer hair cells that provide the work required for the active process (Dallos 1992; Nobili et al. 1998; Ashmore et al. 2000). Although outer hair cell-like motility has not been demonstrated in reptiles and birds, their papillae contain structures analogous to those in the mammalian cochlea such as a basilar membrane. However, one of the most striking anomalies concerning the frog AP is that it lacks a basilar membrane, and yet it clearly demonstrates sharp frequency resolution and sensitivity as well as otoacoustic emissions (OAEs) that are comparable to those found in mammals. In amphibians, reptiles, and birds, the best candidate for an active process may be the active motility of their mechanically sensitive hair bundles (Hudspeth et al. 2000; Fettiplace et al. 2001; Bozovic and Hudspeth 2003).

Although amphibian auditory organs may (Wever 1973) or may not (Will and Fritsch 1988) have arisen independently and separately from those of other vertebrates, studies of these organs provide an opportunity to explore the details of what may be convergent design and function. Do analogous physiological responses arise from similar or different anatomical features? Does the sensory end-organs' fine structure and innervation follow common principles across species? Although there have been extensive investigations into the physiology of these organs, much less is known about the detailed structure of anatomical

correlates of this physiology such as the relationship between conduction velocities and response latencies. Much of the physiology of hair cell and eighth-nerve responses of the AP and BP has been reviewed previously (Lewis and Narins 1999; Smotherman and Narins 2000). Sections 2 and 3 focus on the basic structural correlates of physiological responses of ranid frogs within the auditory papillae and nerve, respectively, and Section 4 focuses on what is known about amphibian OAEs, and discusses the relationship of their properties to the underlying hearing mechanisms as well as the differences between sensory organs.

## 2. AP and BP Sensory Organs

### 2.1 Structural Organization of the AP and BP

Acoustic sense organs attach to the dorsal wall (ceiling) of the AP and BP chambers. In ranid frogs, the AP chamber is oblong and roughly cylindrical. At its lateral end, it opens broadly to the saccule and, towards its medial end, it is closed by a thin contact membrane. As illustrated in Figure 7.2, the hatchet-shaped AP sensory organ can be divided into a rostral patch of hair cells (representing the hatchet blade) up to 30 hair cells wide, an omega-shaped, central curved section (representing the handle neck) with 6 to 10 hair cell rows, and a caudal extension (representing the handle base) that flares out at its caudalmost pole to accommodate 20 rows of hair cells (Wever 1973; Lewis et al. 1985; Simmons et al.

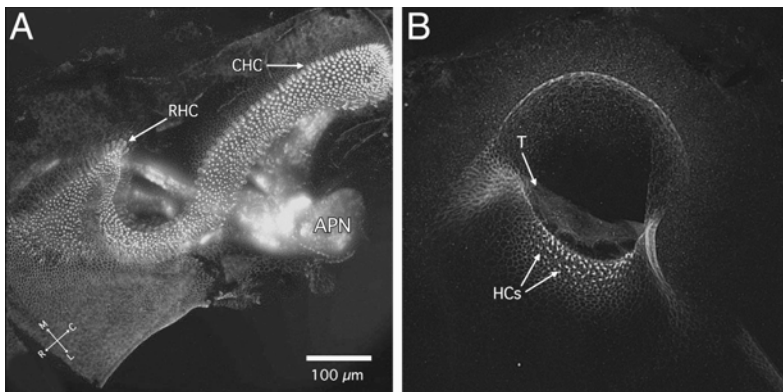


FIGURE 7.2. Confocal images of the amphibian and basilar papillae in the bullfrog. (A) Hair cells in the amphibian papilla (AP) are labeled for myosin VI. A transmission image of the AP nerve is superimposed onto the confocal image of the AP. Rostral (R), lateral (L), and caudal (C) orientations are as indicated. Courtesy of Simmons, Burton, and Baird. (B) Hair cells in the basilar papilla (BP) are labeled with phalloidin. The BP tectorial covering can also be seen. The scale bar in (A) is the same as in (B).

1994b, 2004). Overlying the sensory surface of the AP is a honeycomb meshwork of gelatinous tissue called the tectorium. A thin net of tectorial tissue (tectorial curtain) is suspended across the AP chamber between the AP nerve and the middle region of the AP tectorium. In contrast, the organization of the BP is quite simple. The cylindrical and much smaller BP chamber also opens to the sacculle at its lateral end and is likewise closed by a thin contact membrane towards its medial end. Hair cells in the BP are organized into five or six rows containing up to 20 hair cells each (Wever 1985). The BP has a thin, semi-lunar tectorium stretching across a short tubular passage with an underlying sensory epithelium (Fig. 7.2B). In contrast to the mammalian cochlea, hair cells in both the AP and the BP are rigidly fixed to the cartilaginous wall of the respective papillar recesses, rather than over a flexible membrane. In mammals, traveling waves on the flexible basilar membrane are thought to contribute importantly to the functionality of the cochlea.

There are many features of the frog auditory system that may influence its sensitivity and tuning. The tectorial structures of each papilla, the size of the hair cell, its position within the papilla, as well as its stereovillar morphology all contribute to the thresholds and tuning characteristics of afferent nerve fibers. In addition, the synaptic area and number of synapses per hair cell, the region and number of hair cells innervated, and the diameter and length of each afferent fiber also contribute to the fiber's threshold, latency, and/or tuning responses. However, how the tectorium, hair cells, and synaptic architecture impose limits on eighth-nerve responses is not at all well understood.

For the gross tuning of frog auditory organs, Purgue and Narins (2000a,b) suggest that the frequency difference in neural responses between the AP and BP may be largely explained on the basis of the mechanical tuning of their respective contact membranes. However, only a few studies have attempted to characterize the micromechanics of the tectorium (Lewis and Leverenz 1983; Shofner and Feng 1983; Lewis et al. 1992). With the exception of Wever's hypothesis that the tectorial curtain intercepts the motion of the fluid in the AP chamber and transfers it to the tectorium (Wever 1985), very little is known or has been hypothesized about the dynamics between the point of auditory interception and the initiation of action potentials in the auditory nerve fiber (Smotherman and Narins 2000). In general, the degree to which the fine structure of the auditory end-organ and its nerve fibers are related to physiological parameters such as acoustic tuning, threshold responses, response latencies, and spontaneous activity is not as well understood in frogs as it is in the mammalian cochlea.

## 2.2 *Hair Cell Stereovilli and the Tectorium*

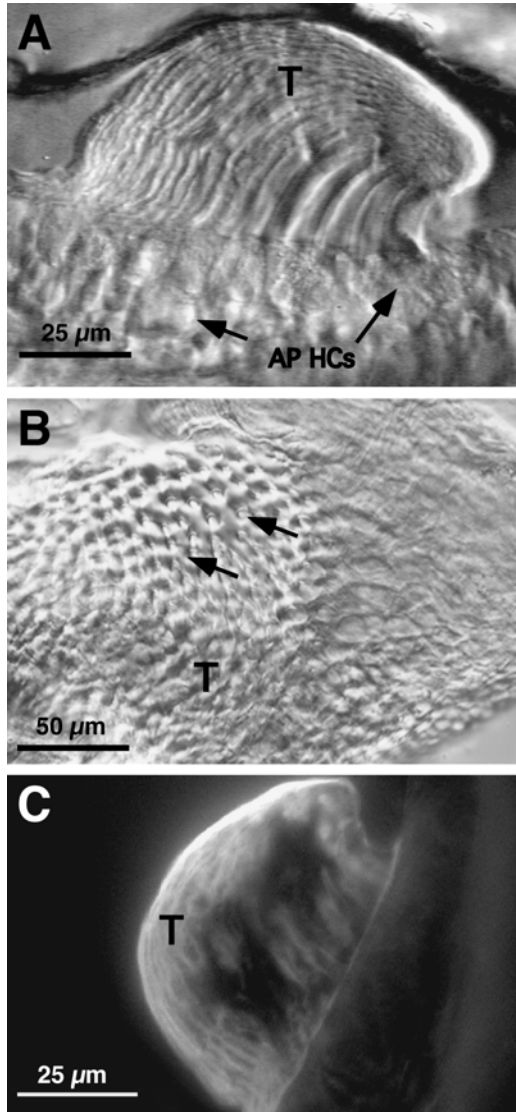
In frogs, auditory hair cells exhibit a variety of distinctive hair bundle morphologies that contain both stereovilli and a true cilium (kinocilium). The hair bundle consists of stereovilli having a graded series of heights with the tallest ones adjacent to the kinocilium. Deflection of the hair bundle towards the kinocil-

ium opens tip-linked transduction channels, resulting in a depolarization of the hair cell. Deflection of the hair bundle away from the kinocilium hyperpolarizes the hair cell. Lewis and colleagues (Lewis and Li 1975; Lewis 1976; Baird and Lewis 1986; Lewis and Lombard 1988) have studied amphibian hair bundles extensively. In general, hair cells on one or more margins of these organs display bundles with an immature or juvenile pattern, suggesting that they make up a marginal growth zone that develops hair cells (Corwin and Warchol 1991; Baird et al. 2000). In contrast to marginal growth zones, hair cells within central regions of the papillae have mature-looking hair bundles. Lewis and colleagues further distinguished at least two categories of mature bundles: those in which the kinocilium extends just beyond the tips of the tallest stereovilli (class 1) and those in which the kinocilium extends well beyond the tallest stereovilli (class 2). Class 1 bundles can be further classified by the presence (1a) or absence (1b) of a conspicuous enlargement or bulb at the tip of the kinocilium and by the bundle height (tall, type E or short, type D).

Hair bundle morphology varies along the transverse axis of the AP, but has not been observed to vary significantly along the (rostrocaudal) axis of tonotopy (Lewis 1976). However, the hair cell polarization (i.e., the orientation of the tallest stereovilli within the bundle) varies along the tonotopic axis, rather than along the transverse direction. Hair bundles rostral to the tectorial curtain (or AP nerve branchlet) are oriented along the rostrocaudal axis, whereas hair bundles caudal to the tectorial curtain are oriented along the transverse (mediolateral) axis of the caudal extension (Lewis and Li 1975; Lewis 1976). Because maximum hair cell response occurs when hair bundles are displaced along their axis of orientation (Flock 1965; Hudspeth and Corey 1977), the optimal stimulus for hair cells requires the tectorium to vibrate along the mediolateral axis in caudal regions and along the rostrocaudal axis in more rostral regions (Lewis and Lombard 1988; Smotherman and Narins 2000). These polarization patterns suggest that the acoustically induced motion of the AP tectorium is complex.

In analogy with the mammalian cochlea, it has been proposed that traveling waves are supported in the AP tectorium (Fig. 7.3). This structure demonstrates a conspicuous tapering in its width and thickness (Shofner and Feng 1984; Lewis and Leverenz 1983). The difference in apparent mass along the tectorium suggests that the thickest portion overlying the rostral AP patch would exhibit larger response latency than the thinnest portion over the caudal AP extension, which would result in a traveling wave. Neurophysiological evidence has suggested that a low-velocity traveling wave exists in the AP (Hillery and Narins 1984, 1987; Lewis 1984). However, a number of studies do not support the idea of a traveling wave along the AP tectorium. For example, Lewis (1988) suggests that the tectorium lacks the appropriate mass and stiffness gradients necessary to support a mammalianlike traveling wave. Anuran DPOAE measurements also argue against the presence of a traveling wave in the AP (Meenderink et al. 2005a) but do support the presence of tectorial disturbances that may lead to OAE generation (Vassilakis et al. 2004).

FIGURE 7.3. (A) Light-micrograph of a transverse section through the tectorial membrane, from a celloidin-embedded section using DIC (Nomarski) optics. (B) Light-micrograph of a horizontal section through the tectorial membrane as it is situated just above the hair bundles. (C) Same section as in A, but with celloidin removed and stained with wheat-germ agglutinin (WGA)-rhodamine and imaged with an epi-fluorescent microscope.



### 2.3 Hair Cell Morphometry

In Figure 7.4, characteristic frequencies (CFs) derived from the bullfrog by Lewis et al. (1982b) and hair cell lengths from studies of the leopard frog by Simmons et al. (1994b) are plotted as a function of normalized distance from the caudal AP pole. In rostral and middle AP regions, hair cell lengths are inversely correlated with a fiber's best frequencies. When moving rostrally, the anterior portion of the rostral AP patch begins around the 80% distance location where hair cell

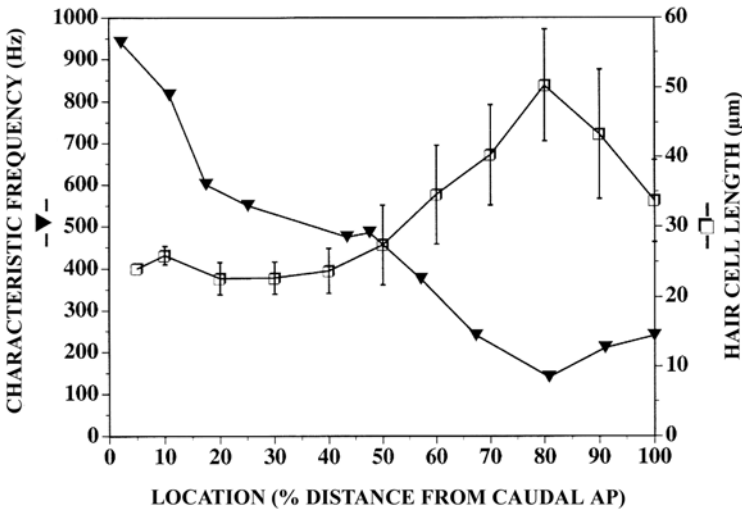


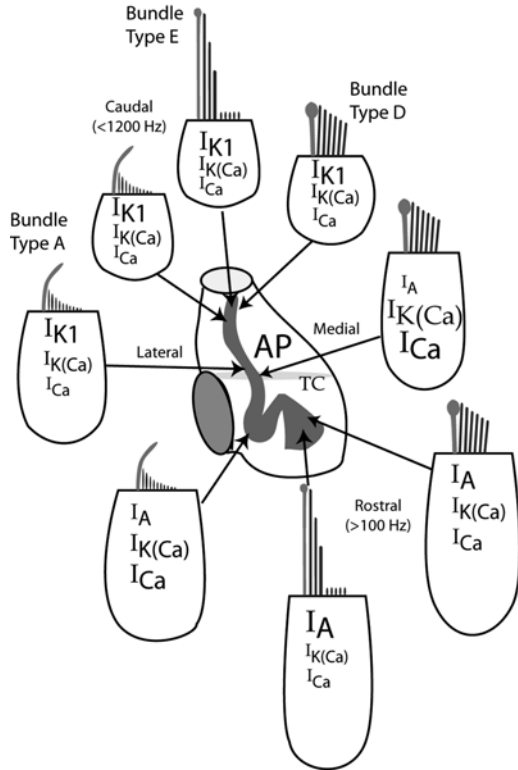
FIGURE 7.4. A plot superimposing the gradient of mean hair cell length in the AP of the leopard frog on the characteristic frequency (CF) tuning gradient in the AP of the bullfrog as determined by Lewis et al. 1982b. From Simmons et al. (1994b).

lengths begin to decrease and where frequencies begin to increase. The relationship between frequencies and hair cell length is less well correlated in the caudal extension. In other vertebrates, inner ear organs also demonstrate an association between hair cell dimensions and tuning. For example, studies of goldfish saccular hair cells reveal morphological gradients similar to those found in the frog AP and further provide evidence for the possibility of hair cell length being related to intrinsic tuning (Sugihara and Furukawa 1989). The pattern of changes in hair cell morphology along the AP rostrocaudal axis correlates well with its observed tonotopy and may have implications for the intrinsic tuning of the AP (Smotherman and Narins 2000). In a study of isolated AP hair cells, Smotherman and Narins (1999a) demonstrated that whole-cell capacitances vary predictably with hair cell body length and thus provided further evidence that the resonant frequency of a hair cell is generally inversely proportional to cell size.

## 2.4 Tuning Properties and Ion Channels

In addition to any mechanical tuning, many nonmammalian hair cells exhibit electrical tuning in which the hair cell's basolateral membrane shows bandpass filtering capabilities. In the frog, hair bundle morphology correlates with a unique set of physiological properties, including transduction sensitivity and rate of adaptation. However, neither bundle height nor bundle type co-varies with CF in any frog auditory organ. Several ionic currents that participate in the electrical

FIGURE 7.5. A schematic diagram of the amphibian papilla chamber in the leopard frog. Within the AP, hair cells show systematic variations in their size, shape, bundle architecture, and membrane electrical properties. The variations in cell size are consistent with cell capacitance changes and relative current amplitudes (represented here by font size). The three principal hair bundle types (A, E, D) are taken from Lewis and Li (1975). The tectorial curtain (TC) is also represented. Reprinted from *J Exp Biol*, 203, MS Smotherman and PM Narins Hair cells, hearing and hopping: a field guide to hair cell physiology in the frog 2237–2246, 2000, with permission from Company of Biologists Ltd.



tuning of AP hair cells have been identified from whole-cell recordings (Fig. 7.5). These include, among others, inward calcium currents and outwardly rectifying potassium currents (Smotherman and Narins 2000). BK channels conduct the major potassium current in hair cells in the bullfrog (Smotherman and Narins 1999b). As a result of these calcium and potassium currents, electrical resonances can be observed in isolated AP hair cells (Pitchford and Ashmore 1987; Smotherman and Narins 1999b) and occur at frequencies very close to the best frequencies of corresponding afferent fibers innervating the AP. Smotherman and Narins (1999a) found that there are two electrically distinct populations of hair cells (rostral and caudal). Within each population, the electrical properties and ionic currents vary along a rostrocaudal gradient. However, electrical tuning mechanisms are only well supported in AP hair cells from the rostral patch. Hair cells from the caudal extension do not appear to be electrically tuned (Smotherman and Narins 1999a). Another related feature of rostral AP hair cells is that they do not possess an inward rectifying  $K^+$  current ( $I_{K1}$  in Fig. 7.5). The unique absence of these channels in the rostral AP patch is consistent with the role of this ionic current in elevating auditory nerve thresholds by a reduction in neurotransmitter release (Smotherman and Narins 2000).

## 2.5 Synaptic Ultrastructure

The ultrastructure of synapses on hair cells in the AP is, according to several studies, consistent with other rostrocaudal gradients. Early ultrastructural studies predicted there might be a rostrocaudal gradient in synaptic architecture but provided no detailed evidence for such (Flock and Flock 1966; Frishkopf and Flock 1974). Studies of the ultrastructural characteristics of synapses and nerve fibers in both rostral and caudal regions of the AP have shown that hair cells in the rostral patch region differ significantly in their synaptic architecture from hair cells in the caudal extension (Simmons et al. 1995; Fig. 7.6A). Additionally, reconstructions of synaptic complexes suggest significant differences in the number of synaptic sites between rostral and caudal locations on tall and short hair cells, respectively. Both the number of synaptic sites and the amount of neurotransmitter released have been associated with the efficacy of synaptic transmission and subsequent nerve fiber responses. Thus, the ultrastructural data are consistent with the hypothesis that a hair cell's innervation pattern is related to specific features of auditory nerve fiber responses such as their spontaneous activity, thresholds, and their ability to follow rapid temporal variations in the stimulus.

Hair cell afferent synapses are known as ribbon synapses, and their structure has been well documented across most vertebrates (Smith and Sjostrand 1961; Gleisner et al. 1973; Liberman 1980; Sobkowicz et al. 1986; Chang et al. 1992; Simmons et al. 1994a, 1995; Lenzi et al. 1999). Similar to descriptions in other inner ear organs (Gleisner et al. 1973; Frishkopf and Flock 1974; Liberman et al. 1990; Chang et al. 1992), AP hair cell ribbon synapses contain a dense, spherical-to-elliptical presynaptic body, surrounded by a halo of tethered synaptic vesicles (Fig. F.6B). The ribbon or presynaptic body is typically seen in close apposition to the synaptic active zone that contains docked vesicles and  $\text{Ca}^{2+}$  entry sites for  $\text{Ca}^{2+}$ -induced exocytosis (Zenisek et al. 2003).

The most complete ultrastructural studies of the hair cell ribbon synapse in amphibians are from the bullfrog saccule (Lenzi et al. 1999) and the leopard frog AP (Simmons et al. 1995). In the leopard frog, each hair cell makes a synapse with several terminals, and afferent fibers appear to innervate several hair cells via *en passant* contacts. Simmons et al. (1995) reconstructed afferent ribbon synapses from serial thin sections and demonstrated a clear rostrocaudal gradient in the size of the presynaptic ribbon. In this study, significant differences were found in the innervation and synaptic ultrastructure between hair cells with tall (type E) bundles and those with short (type D) bundles in the rostral and caudal portions of the AP.

Studies at the neuromuscular junction suggest that the number and distribution of active zone particles at an active zone determines the probability of transmitter release at that site (Walrond and Reese 1985; Lnenicka et al. 1986). However, observations in the mammalian inner ear suggest just the opposite may be the case (Liberman et al. 1990). Presynaptic body size appears to be inversely related to fiber diameter and spontaneous rate. This discrepancy may simply reflect an

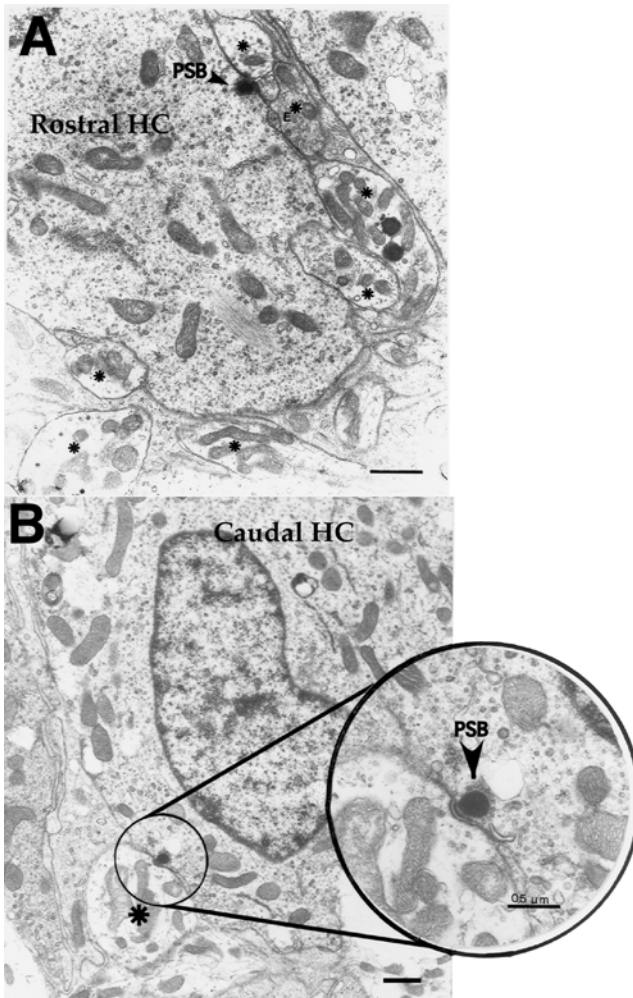


FIGURE 7.6. (A) Transmission electron micrograph (TEM) of a cross-section through the synaptic pole of a rostrally located tall hair cell (HC). Both afferent and efferent terminals are identified with asterisks. A hair cell presynaptic body (PSB) is opposite one of the afferent terminals. In the region shown, there are five afferent terminals and one efferent (E) terminal contacting the basal portion of the HC. (B) TEM of a cross-section through the synaptic pole of a caudally located short HC. In this micrograph, the caudal HC has just one afferent terminal (asterisk) in synaptic contact. This section is midway through the synaptic site. The inset shows the synaptic site with its PSB at higher magnification. Adapted from Simmons et al. (1995). Scale bars in (A) and (B) represent 10 $\mu$ m.

inadequate understanding of the presynaptic body and its functional significance. Although the exact role of a morphological parameter such as synaptic ultrastructure in sculpting the physiological responses of the auditory nerve fibers is unknown, it is likely to correlate with the spatial and temporal analysis resolution applied to the incoming stimulus.

Few hair cell organs lack efferent synapses, the basilar papilla of the frog being one (Frishkopf and Flock 1974). Flock and Flock (1966) reported that efferent-type terminals were more abundant on rostral AP hair cells than on caudal AP hair cells. In a more detailed study of hair cell synapses, Simmons et al. (1995) found densely packed, vesiculated efferent terminals mostly on the tall hair cells in the rostral AP patch (Fig. 7.6A). Rostral hair cells are contacted by at least one and as many as three efferent terminals. Efferent terminals have punctate swellings rather than being *en passant* fibers, characteristic of the majority of the afferent terminals. Although generally smaller, efferent terminals can be as large as afferent terminals with diameters generally ranging from 0.2 to 2.0  $\mu\text{m}$ .

### 3. AP and BP Nerve Fibers

#### 3.1 AP and BP Nerve Fiber Responses

By selectively lesioning the eighth-nerve branchlets innervating individual sensory maculae within the otic capsule of the bullfrog inner ear, it was demonstrated that fibers tuned to low- and mid-frequencies innervate the AP and fibers tuned to higher frequencies innervate the BP (Feng et al. 1975). Subsequent studies assumed that similar organization held for other frog species (Capranica and Moffat 1975, 1983; Capranica 1978; Zakon and Capranica 1981; Narins 1983; Hödl et al. 2004). The only neurophysiologically derived tonotopic map available for any amphibian is for the bullfrog, *R. catesbeiana* (Lewis et al. 1982a,b). In the bullfrog AP, nerve fibers innervating the rostral AP patch exhibit CFs between 100 and 300 Hz. Fibers that innervate the caudal extension exhibit CFs roughly between 400 and 1000 Hz. Nerve fibers innervating the bullfrog BP have CFs between 1000 and 3000 Hz without any apparent tonotopy.

Typically, frog auditory nerve fibers are characterized in the frequency domain by frequency tuning curves (FTC), that is, a plot of their response threshold to a sinusoidal input (typically in decibels SPL, or re 0.0002 dynes/cm<sup>2</sup>) as a function of the input frequency. Each fiber has its lowest threshold to one (characteristic) frequency (CF) and behaves as a bandpass filter; that is, its threshold rises as the stimulus frequency deviates in either direction from CF. The tuning curves of frog auditory nerve fibers are V-shaped when plotted on a log-log scale. The FTC shape (i.e., the relative degree of sharpness) reflects the underlying tuning mechanisms. In the frog, the sharpness of tuning as measured by the  $Q_{10\text{dB}}$  decreases with CF (Ronken 1990, 1991; Stiebler and Narins 1990). In the AP, afferent fibers with low CFs (rostral regions) have  $Q_{10\text{dB}}$  values as high as 5. Afferent fibers with high CFs from either caudal AP regions or the BP are more broadly tuned and

rarely exceed a  $Q_{10dB}$  value of 2. Auditory nerve fibers in frogs exhibit similar frequency selectivity to that in mammals for the same CF despite clear anatomical differences between the ears of the two groups.

In addition to characterizing auditory nerve fiber responses by their frequency functions (i.e., tuning curves), a linear systems approach can be used to characterize nerve fiber responses to continuous broadband noise in the time domain by applying Wiener kernel analysis. Basically, a series of Wiener kernels characterizes a linear system that describes the (nonlinear) signal path between auditory input and neural output. This series can be determined experimentally by calculating the reverse correlation between a continuous, Gaussian noise stimulus and the ear's response to this stimulus, that is, the occurrence of spikes in the auditory nerve fiber (Schetzen 1989). Wiener kernel analysis reveals amplitude and phase characteristics of single nerve fiber responses (Eggermont 1993; van Dijk et al. 1994; Lewis et al. 2002; Lewis and van Dijk 2004). The first-order Wiener kernel is obtained by averaging the stimulus windows preceding each spike in the nerve fiber response. It is proportional to the reverse correlation (REVCOR) function of auditory nerve fibers and reveals the linear response of a system such as the ear (De Boer 1967; van Dijk et al. 1994). The second-order Wiener kernel is also calculated from the stimulus windows preceding neural spikes and provides (1) a two-dimensional visual image of a fiber's second-order nonlinear dynamics and (2) information about a fiber's tuning and timing of excitation, adaptation, and suppression responses (Lewis et al. 2002; Lewis and van Dijk 2004). Further analysis of Wiener kernels has provided qualitative information on the auditory filters and the interaction (tuning and timing) between suppression and excitation within the auditory nerve (Lewis and van Dijk, 2004). Most studies have been limited to the calculation of the first- and/or second-order Wiener kernel, although higher-order kernels may exist (e.g., van Dijk 1995), thus reflecting the presence of higher-order nonlinearities within the anuran inner ear.

In ranid frogs, AP and BP nerve fibers not only differ in their frequency tuning, but also in their temperature dependence, spontaneous activity, threshold and intensity responses, and OAEs. Table 7.1 summarizes many of the physiological characteristics of auditory nerve fibers found in anuran species. Although the extent of the frequency range in the AP varies with species, its properties are relatively uniform across groups (Zakon and Wilczynski 1988). The range of frequencies (at or below 100 Hz up to 1.0–1.4 kHz) represented along the AP sensory organ is correlated with the length of the caudal extension across species (Feng and Shofner 1981; Lewis 1981). Additionally, low-CF fibers show two-tone suppression, that is, reduction of a fiber's response to a tone by another tone of higher frequency (Liff and Goldstein 1970; Ehret et al. 1983; Rose and Capranica 1985; Christensen-Dalsgaard et al. 1998), or of lower frequency (Benedix et al. 1994). Two-tone suppression is not found in mid- or high-CF fibers. However, one-tone suppression (spontaneous activity suppressed by a single tone) may be a more general phenomenon within the AP (Christensen-Dalsgaard and Jørgensen 1996). The CFs of auditory nerve fibers from the AP also show a temperature

TABLE 7.1. Summary of peripheral auditory nerve physiology.

Parameter	AP rostral	AP caudal	BP	Possible anatomical correlate(s)	References
<b>FREQUENCY CHARACTERISTICS</b>					
Frequency tuning (Hz)	~100–400 Hz	~400–1000 Hz up to 1.4 kHz	>1000 Hz	Tectorium, hair bundle, hair cell locations	Feng et al. 1975 Feng and Shofner 1981 Lewis 1981 Zakon and Wilczynski 1988 Lewis et al. 1982a,b
Tonotopic organization	Decreasing (300 to 100 Hz) Increasing (100 to 400 Hz) Broad (as high as 4–5)	Increasing (400 to 1000 Hz)	None	Tectorium, hair bundle, hair cell locations	
Tuning sharpness, $Q_{10, dB}$		Sharp (typically $\leq 2$ )	Typically $\leq 2$	Tectorium, Innervation pattern	Ronken 1990, 1991 Stiebler and Narins 1990 Capranica and Moffat 1983
Minimum threshold sensitivity to tones (dB SPL)	~30–90 dB SPL	~40–90 dB SPL	~50–80 dB SPL	Hair cell innervation density	
Tone suppression	Present	None	None	Tectorium, hair bundle	Ehret et al. 1983 Rose and Capranica 1985 Christensen-Dalsgaard and Jørgensen 1996 Christensen-Dalsgaard et al. 1998

TABLE 7.1. *Continued*

Parameter	AP rostral	AP caudal	BP	Possible anatomical correlate(s)	References
Phase locking	Strong	Moderate	Weak	Tectorium, hair bundle	Dunia and Narins 1989 Simmons et al. 1993
<b>TEMPORAL CHARACTERISTICS</b>					
Spontaneous rates (spikes/s)	0–80/s	0–50/s	0–40/s	Hair bundle, number of synapses	Ronken 1990 Christensen-Dalsgaard et al. 1998
Dynamic range (dB)	≤50dB	≤30dB	20–30dB	Hair bundle, number of synapses	Capranica and Moffat 1983
Response (click) latency (ms)	Up to 8 ms	2–5 ms	2–3 ms	Tectorium, hair bundle, fiber diameter	Hillery and Narins 1984, 1987
Amplitude modulation response	Present	Present	Present	Tectorium, hair bundle	Simmons 1988
Temperature sensitivity	Present	Present in lower frequencies	None	Hair cell (electrical tuning)	Simmons et al. 1993 Stiebler and Narins 1990 van Dijk et al. 1990
Sexual dimorphism	None	None	Present		Narins and Capranica 1976
Size differences	None	None	Present		Wilezynski et al. 1992

dependence: lowering the animal's core temperature decreases a fiber's CF (Stiebler and Narins 1990; van Dijk et al. 1990). Although BP nerve fibers are typically tuned to frequencies  $>1.0$  kHz and to a narrow range of CFs, tuning characteristics of nerve fibers are species-specific and, within a species, can vary with size, sex, or geographical location (Narins and Capranica 1976; Capranica 1978; Capranica and Moffat 1983). As a rule, the BP of large-sized species is tuned to lower frequencies than that of smaller-sized species and males have BPs tuned to generally higher frequencies than females (Narins and Capranica 1976; Wilczynski et al. 1992, 1993). Auditory nerve fibers of the BP show little or no change in their physiological properties when the animal's temperature is experimentally varied (Stiebler and Narins 1990; van Dijk et al. 1990, 1997; Carey and Zelick 1993; Benedix et al. 1994).

Auditory nerve fibers in the frog exhibit spontaneous activity, although reports as to the exact level vary widely based on the methods and species used. Earlier reports of spontaneous activity suggested that low-CF fibers generally have the lowest spontaneous rates, typically less than five spikes per second, whereas higher-CF fibers generally have higher spontaneous rates (Feng et al. 1975; Capranica 1978; Capranica and Moffat 1980, 1983; Zelick and Narins 1985; Ronken 1990; Ronken et al. 1993). However, more recent reports (Christensen-Dalsgaard et al. 1998) find no correlation between spontaneous activity and CF, but between spontaneous activity and threshold (fibers with low threshold responses to sounds tend to have higher spontaneous rates). Interestingly, low auditory thresholds in the frog have also been correlated with high DPOAE amplitudes (van Dijk et al. 2002; Vassilakis et al. 2004; and see Section 4.3.).

### *3.2 Fiber Morphometry, Conduction Velocity, and Response Latency*

The physiological parameters of amphibian auditory nerve fibers can be defined by a structural unit that includes the tectorial membrane, the hair cells innervated by a single neuron, and the synaptic architecture and pattern of afferent innervation. However, how the anatomical patterns of hair cells and synaptic arrangements affect physiological responses is poorly understood. It has been tempting to associate such patterns with the observed physiological distribution of primary axons: low frequency, suppressible units, and mid-frequency, nonsuppressible units (Feng et al. 1975; Lewis 1976; Smotherman and Narins 2000).

In auditory organs, one of the best-characterized examples of structure–function relationships has been in the mammalian cochlea, where different spontaneous rate categories of auditory afferent fibers have been correlated with the size, location on the hair cell, synaptic arrangement, and mitochondrial content of nerve fiber terminals (Lieberman 1980; Liberman and Simmons 1985; Gleich and Wilson 1993). To date, structure–function relationships have not been investigated at the same level of detail in the frog.

The innervation patterns of individual auditory neurons within AP and BP organs have been reconstructed in both leopard frogs and bullfrogs (Lewis et al.

1982b; Simmons et al. 1992). Most notably, the innervation of both AP and BP organs is highly convergent; that is, individual neurons make synaptic contact with multiple hair cells. Nerve fibers in the AP terminate on varying numbers of receptor hair cells (Simmons et al. 1992), with the physiological gradients following roughly the rostrocaudal gradient of hair cell innervation (Lewis et al. 1982b; Simmons et al. 1994b, 1995). Nerve fibers that respond best to lower frequencies contact more hair cells than fibers that respond best to higher frequencies. Retrograde-labeling studies suggest that (1) response latencies and conduction velocities may be correlated with the papillar location as well as the number of hair cells innervated and afferent fiber size (Lewis et al. 1982b; Simmons et al. 1992) and (2) the pattern of hair cell innervation may in part determine physiological parameters of auditory nerve fiber responses such as tuning sharpness and sensitivity. For example, large innervation areas (i.e., dendritic fields) might be correlated with broad tuning observed in a given auditory nerve fiber and quite possibly with poor frequency resolution.

### *3.3 AP Nerve Structural Correlates*

Nerve fibers terminating in the caudal (high-frequency) end of the AP have smaller diameters than fibers terminating in the rostral (low frequency) end of the AP (Simmons et al. 1992; Simmons and Narins 1995). Both caudal and rostral AP fibers have nearly equal lengths from the ganglion to their terminations and virtually all of the fibers are myelinated (average  $\pm$  s.d. myelin thickness of  $0.13 \pm 0.05 \mu\text{m}$ ; Simmons and Narins 1995). Larger diameter fibers appear more heavily myelinated and are situated within the center of the nerve bundle. These data suggest that fiber size is directly correlated with the area of innervation. In combination with previous neurophysiological results (Hillery and Narins 1984, 1987), such differences in fiber size may also relate to the differences found in response latencies to click stimuli (Hau et al. 2004).

The relationship between fiber morphometry and conduction velocity may play a significant role in understanding response latencies. Auditory nerve latency is an important feature of the acoustic transformation process and may encode additional information about the acoustic stimuli, including the directionality and periodicity of the source of sound (Bleeck and Langner 2001). In the frog AP as well as the mammalian cochlea, auditory nerve fibers that respond best to high-frequency stimuli have short response latencies and nerve fibers that respond best to low-frequency stimuli have longer response latencies (Kiang et al. 1965; Hillery and Narins 1987; Fitzgerald et al. 2001; Hau et al. 2004). In mammals, this observation has been linked to the traveling wave transit time along the basilar membrane in addition to the differences in path length between high-frequency (with short distances to the brain) and low-frequency (with longer distances to the brain) fibers. Although a similar latency–frequency relationship exists in the frog AP, this organ neither has a basilar membrane nor exhibits a significant difference in path length between high- and low-frequency fibers. However, an observation not suspected to play a significant role in

mammalian response latencies is that frog auditory nerve fibers responding to high frequencies are typically thin and fibers responding to lower frequencies are thicker.

Previous theoretical studies of conduction velocities in nerve fibers (Rushton 1951; Deutsch 1969; Smith and Koles 1970) indicate that myelin thickness in nerve fibers is such that, for a fiber of given external diameter, conduction velocity is maximized. For fibers with the same myelin thickness, fibers with large diameters conduct impulses faster. Based on preliminary estimates of theoretical conduction velocities [velocity =  $k$  (diameter)], rostral AP fibers should have the highest conduction velocity, caudal AP fibers should have low conduction velocities, and BP fibers should have a range of conduction velocities. The difference between theoretical estimates and measured latencies suggests that other variables may be involved in determining response latencies. Two such variables are the time it takes an acoustic signal to stimulate hair cell stereovilli and the time it takes hair cells, once stimulated, to give rise to action potentials in auditory nerve fibers (Hau, Simmons, and Narins 2005, unpublished data).

The tectorium may also contribute to the response latencies observed in AP nerve fibers, as it is a complex gelatinous structure with its most massive segment overlying the rostral AP patch (Shofner and Feng 1983; Hau et al. 2004). A traveling wave across the tectorium would be expected to stimulate higher-frequency regions before lower-frequency regions by as much as a factor of 10 and would be consistent with the observed longer latencies of rostrally innervating fibers.

## 4. Otoacoustic Emissions

### 4.1 Introduction

One of the remarkable properties of the vertebrate inner ear is its great sensitivity. From early on it was recognized that such sensitivity could not arise solely from passive responses to sound. Rather, some active amplification mechanism would be required to enhance the vibration of inner ear structures in response to low-level acoustic stimuli (Gold 1948). In mammals, this mechanism has been linked to outer hair cell (OHC) motility and receptor potential (see reviews by Probst et al. 1991 and Robles and Ruggero 2001) and is termed the “cochlear amplifier” (Davis 1983). It utilizes bioelectrochemical energy (Zheng et al. 2000; Liberman et al. 2002), which may propagate through the middle ear to the outside in the form of vibrations in the hearing frequency range. The discovery of low-level sounds corresponding to such vibrations (Kemp 1978) provided the first evidence for the presence of an active amplification mechanism within the inner ear. These sounds are now known as OAEs and can be measured by placing a sensitive microphone in the ear canal.

Since their discovery in mammals, OAEs have been reported to be present in all classes of terrestrial vertebrates (Köppl 1995; Köppl and Authier 1995), sug-

gesting that they reflect a fundamental property of normal hearing. Because OAEs can be recorded noninvasively, they provide an important tool to hearing researchers. OAEs are often used for diagnostic screening of frequency-dependent cochlear function (Lonsbury-Martin et al. 1993; Stover et al. 1996; Wagner and Plinkert 1999; Abdala 2000; Emmerich et al. 2000) or middle ear damage (Owens et al. 1992, 1993; Zhang and Abbas 1997). In addition, OAEs provide a noninvasive means of examining inner ear mechanisms in mammals (Kössl and Vater 1996; Maison et al. 1997; Shera and Guinan 1999) and other vertebrates (Rosowski et al. 1984; Vassilakis et al. 2004), as well as in insects (Kössl and Boyan 1998).

Traditionally, OAEs have been classified into spontaneous OAEs (SOAEs) and evoked OAEs (EOAEs), based on whether an external stimulus is required for their generation. Furthermore, based on the type of stimulus required for their generation, EOAEs are classified into (1) stimulus-frequency OAEs or SFOAEs (evoked by single sinusoidal stimuli), (2) transient-evoked OAEs or TEOAEs (evoked by short-duration, low-level signals of various spectra), and (3) distortion-product OAEs or DPOAEs (evoked by two continuous sinusoidal stimuli) (Probst et al. 1991). It has been argued that the above classifications do not do justice to the mechanisms underlying OAE generation (Shera and Guinan 1999; Kalluri and Shera 2001). However for the sake of consistency, the traditional classification scheme is presented. Both the AP and BP exhibit OAEs but their properties differ considerably.

## 4.2 *Stimulus-Frequency and Transient-Evoked Otoacoustic Emissions*

Upon stimulation with single continuous sinusoids or short signals of various spectral distributions (e.g., clicks), the inner ear generates SFOAEs or TEOAEs, respectively, which coincide in frequency with the component(s) of the external stimulus. It is currently believed that both SFOAEs and TEOAEs arise from the same inner ear mechanism. Unfortunately, the number of studies exploring these types of OAEs in frogs is limited.

Whitehead et al. (1986) examined SFOAEs and their relationship to body temperature in *Rana temporaria*. The authors were able to evoke SFOAEs only for frequencies below 1 kHz, suggesting that in this species, SFOAEs may arise only from the AP. Palmer and Wilson (1982) were able to evoke measurable SFOAEs in *Rana esculenta* for frequencies up to 2 kHz, implying that in this species, both papillae generate SFOAEs. The effect of body temperature on SFOAE frequencies is very pronounced, suggesting that SFOAE generation may involve an electrochemical tuning mechanism along, possibly, with some form of mechanical tuning. In addition, SFOAE levels increase just before the start of the frog breeding season (Whitehead et al. 1986), suggesting that OAE generation in frogs may be seasonal and under hormonal control.

TEOAEs were reported by Palmer and Wilson (1982) but not in enough detail to support an account of TEOAE-properties.

### 4.3 Distortion-Product Otoacoustic Emissions (DPOAEs)

Upon stimulation with two continuous sinusoids (often termed primaries) of appropriately chosen frequencies ( $f_1, f_2$ , where  $f_2 > f_1$ ) and intensities ( $L_1, L_2$ ), the inner ear generates DPOAEs. DPOAE frequencies coincide with the intermodulation distortion frequencies of the two primaries, whereas the most-studied DPOAEs coincide in frequency with the third-order intermodulation distortion frequencies ( $2f_1 - f_2$  and  $2f_2 - f_1$ ). As such, DPOAEs are the only type of EOAEs that do not match in frequency any of the frequencies present in the external stimulus, a fortunate property that simplifies their study.

With the exception of early reports (Baker et al. 1989), DPOAEs have been recorded in frog species from the families Ranidae, Hylidae, and Pipidae (van Dijk and Manley 2001; van Dijk et al. 2002, 2003; Meenderink and van Dijk 2004, 2005a; Vassilakis et al. 2004; Meenderink et al. 2005a,b). No DPOAEs were found in species from the families Bombinatoridae and Pelobatidae (van Dijk et al. 2002). It is thought this apparent difference between frogs from different families is related to the overall sensitivity of the hearing apparatus (van Dijk et al. 2002).

The amplitude and phase of DPOAEs depends on the parameters that describe the two primaries. These parameters outline a four-dimensional parameter space usually defined by  $f_1, f_2/f_1, L_1$ , and  $L_1 - L_2$ . In general, individual studies limit their exploration to isolated slices/planes within this space. When the two primary frequencies are systematically varied (i.e., changes only in the  $f_1$  dimension of the parameter space), plotting DPOAE amplitude versus frequency results in a DPOAE-audiogram. In frogs, DPOAE-audiograms typically exhibit two maxima; one below and one above approximately 1 kHz (Fig. 7.7). It is currently believed that the bimodal shape of frog DPOAE-audiograms reflects emission generation from the two papillae, with the low- and high-frequency peaks representing DPOAEs generated within the AP and the BP, respectively. This bimodality seems to be independent of both the primary frequency ratio (van Dijk and Manley 2001; Meenderink et al. 2005a) and the absolute levels of the primaries (Meenderink and van Dijk 2004). DPOAEs from the AP (AP-DPOAEs) and the BP (BP-DPOAEs) differ in several respects and are referred to separately.

DPOAE-audiogram data can be extended by recording multiple DPOAE audiograms from the same animal, each with a different  $f_2/f_1$  (Fig. 7.8). The resulting ( $f_1, f_2$ ) area maps reveal DPOAE amplitude and phase patterns that are different from those obtained from the mammalian cochlea (Knight and Kemp 2000; Schneider et al. 2003). A transmission-line model that incorporates cochlear properties such as traveling waves may explain the mammalian DPOAE patterns (Knight and Kemp 2001). In contrast, the frog patterns obtained from both the AP and the BP may be modeled by a single nonlinearity, suggesting the absence of mammalianlike traveling waves (Meenderink et al. 2005a). Several mammalian studies (e.g., Shera and Guinan 1999; Faulstich and Kössl 2000) have argued that  $f_2/f_1$  must be  $\geq 1.15$ , to avoid phase complications (e.g., rapidly rotating phase and regular amplitude variations of the DPOAEs, due to beating

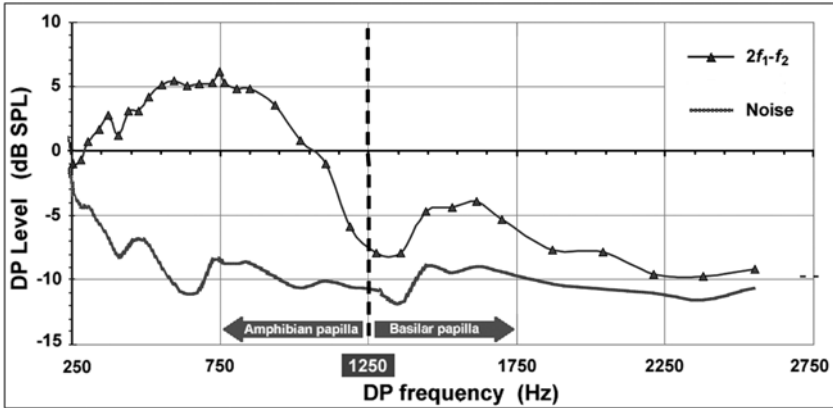


FIGURE 7.7. Average levels of the  $2f_1-f_2$  ( $\blacktriangle$ ) DPOAE from *R. p. pipiens* (20 ears: both ears of five males and five females) for  $f_2/f_1 = 1.15$ ,  $L_1 = L_2 = 60$  dB SPL ( $\pm 2.5$  dB), and  $240 \geq f_1 \geq 3000$  Hz as a function of DP frequency. The dashed vertical line marks the “break” in the frequency coverage of the AP and the BP (1250 Hz). Adapted from Vassilakis et al. (2004).

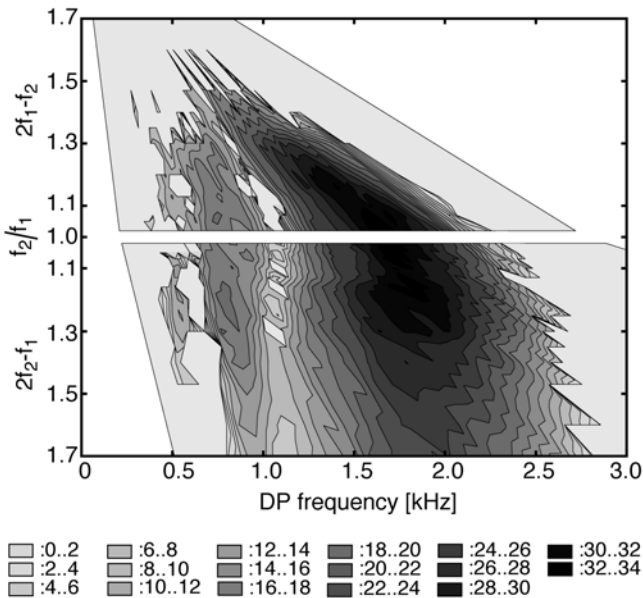


FIGURE 7.8. DPOAE amplitudes (levels given in the key) at  $2f_1-f_2$  and  $2f_2-f_1$  in dB SPL, evoked with  $L_1 = L_2 = 76$  dB SPL. Data are plotted as  $f_2/f_1$  versus DP frequency. Contour lines are drawn at 2 dB intervals. From Meenderink et al. (2005a).

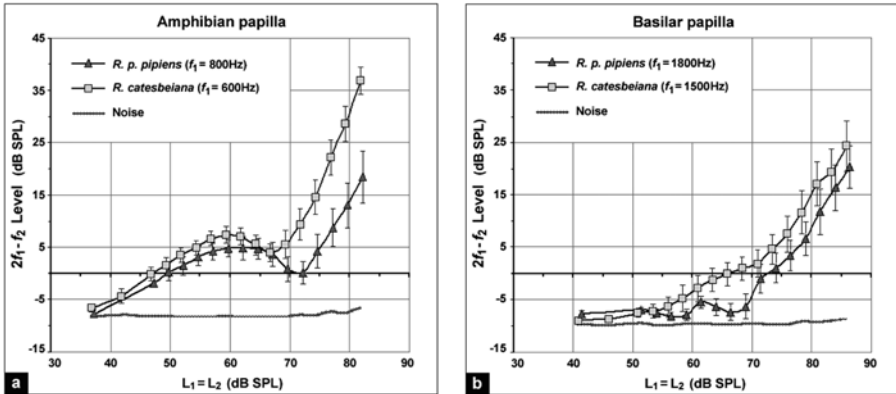


FIGURE 7.9. DPOAE I/O curves for  $f_2/f_1 = 1.15$  from *R. p. pipiens* ( $\blacktriangle$ ,  $f_1 = 800$  Hz, 1800 Hz) and *R. catesbeiana* ( $\square$ ,  $f_1 = 600$  Hz, 1500 Hz). Average DPOAE levels ( $2f_1 - f_2$ ) and standard errors (20 ears each species: both ears of five males and five females). (A) AP; (B) BP. Adapted from Vassilakis et al. (2004).

between the primaries) that arise as  $f_2/f_1$  drops below 1.1. Consistent with filtering mechanism and two-tone suppression differences between the mammalian and the frog inner ears, no such complications arise for low  $f_2/f_1$  values in the frog (van Dijk and Manley 2001; Meenderink et al. 2005a).

The relationship of DPOAE amplitude to the absolute levels of the primaries (i.e., to changes in both stimulus levels with  $L_1 - L_2 = 0$ ) is most commonly visualized in the form of DPOAE input/output curves (I/O curves). For  $L_1 = L_2 < \sim 70$  dB SPL, the growth rate of the AP-DPOAE I/O curves is compressive (i.e.,  $\leq 1$  dB/dB), whereas for higher primary levels ( $L_1 = L_2 > \sim 70$  dB SPL) it is expansive (i.e., 2 to 3 dB/dB; Fig. 7.9A). The growth rate of the BP-DPOAE I/O curves does not appear to vary with absolute primary levels, but remains expansive (i.e., 2 to 3 dB/dB) over the entire stimulus level range tested (Meenderink and van Dijk 2004; Vassilakis et al. 2004; Fig. 7.9B).

Recording DPOAEs for unequal primary levels provides a more complete picture of DPOAE-dependence on  $L_1$  and  $L_2$ . For low-to-moderate primary levels and relatively small frequency ratios ( $f_2/f_1 \leq 1.15$ ), maximum DPOAE amplitudes are obtained for  $L_1 - L_2 \approx 0$  in both the AP (Vassilakis et al. 2004; Meenderink and van Dijk 2005a; Fig. 7.10). For larger frequency ratios (e.g.,  $f_2/f_1 = 1.3$ ), the primary level difference ( $L_1 - L_2$ ) resulting in maximum BP-DPOAE amplitude (i.e., optimal level difference) varies with primary frequencies (Meenderink and van Dijk 2005a). In mammals, the relationship of this optimal level difference ( $L_1 - L_2$ ) to the absolute primary levels ( $L_1, L_2$ ) and the relative primary frequencies ( $f_2/f_1$ ) may be explained in terms of basilar membrane disturbance envelopes (e.g., Kummer et al. 2000). It has been argued that the difference in these relationships between mammals and frogs may be related to differences in

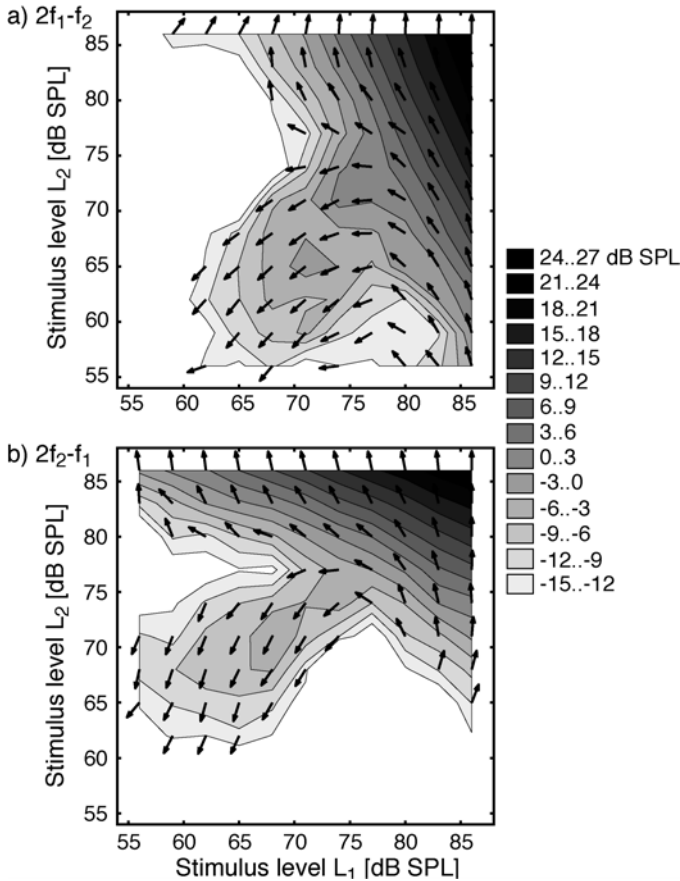


FIGURE 7.10. Amplitude and phase of DPOAEs at (A)  $2f_1-f_2$  and (B)  $2f_2-f_1$  as a function of stimulus levels ( $L_1$ ,  $L_2$ ). Due to the stimulus parameters used ( $f_1 = 1913\text{ Hz}$ ;  $f_2/f_1 = 1.1$ ), the resulting DPOAEs originate in the BP. Contour lines (drawn at 3 dB intervals) represent amplitude (levels given in the key) and arrows represent phase. Phase is relative to the phase at  $L_1 = L_2 = 86\text{ dB SPL}$ . From Meenderink and van Dijk (2005).

the mechanical tuning properties of the mammalian basilar membrane and the frog tectorium (Vassilakis et al. 2004).

AP- and BP-DPOAEs arising in response to low-level primaries also differ in their vulnerability to physiological insults (van Dijk et al. 2003) and to changes in body temperature (Meenderink and van Dijk 2005b). AP-DPOAEs rapidly disappear when oxygen supply is hindered or when body temperature is decreased. In contrast, anoxia takes much longer to influence BP-DPOAEs, whereas temperature changes have no clear effect.

It is currently believed that DPOAEs result from the combination of two level-dependent DPOAE components (Whitehead et al. 1992). The first component dominates for low-level primaries, saturating as primary levels increase. The

second component dominates for high-level primaries, with its amplitude dropping below that of the low-level component as primary levels decrease. A phase difference of  $\sim\pi$  rad between these two components is believed to be responsible for the DPOAE I/O-curve notches observed for intermediate primary levels (Mills and Rubel 1994). In contrast to mammalian data, this phase difference increases systematically from 0 to  $\pi$  rad with increasing primary frequencies in both frog papillae (Meenderink and van Dijk 2004).

Vassilakis et al. (2004) compared the frequency ranges of the AP and BP response with DPOAE-audiograms plotted as functions of  $f_1$ ,  $f_2$ , and DP frequency, and interpreted their degree of correlation as providing evidence for the site of DPOAE-generation. Opposite to mammals, they found that the generation of the  $2f_1-f_2$  DPOAE in the frog may primarily occur at or near the DPOAE frequency place, whereas the generation of the  $2f_2-f_1$  DPOAE may primarily occur at a frequency place between the two primaries. This opposite behavior may be related to various anatomical differences between the mammalian and frog ears, including the absence, in the frog ear, of a basilar membrane, and may be a manifestation of differences regarding the possibility of traveling wave development.

The single study exploring sex differences in frog DPOAEs (Vassilakis et al. 2004) indicates that, although overall frog DPOAE generation mechanisms may be independent of sex, females produce stronger emissions than males, from both the AP and the BP (Fig. 7.11). This difference is consistent with mammalian results and may be related to sex differences in frog ear frequency tuning, sensitivity (Narins and Capranica 1976), and middle- and inner-ear physiology (Mason et al. 2003).

#### 4.4 *Spontaneous Otoacoustic Emissions (SOAEs)*

As is clear from their name, SOAEs arise spontaneously, without the need of an external evoking stimulus. The peaks in the frequency spectrum corresponding to SOAEs can be identified by (a) their consistent presence in the average of a large number of spectra, (b) their susceptibility to changes in temperature, and (c) their modification (suppression and frequency modulation) by external tones. SOAEs have been reported for frog species in the families Ranidae, Hylidae, and Leptodactylidae (Baker et al. 1989; van Dijk et al. 1996), but not for species in the families Pipidae and Bombinatoridae (van Dijk et al. 1996). They have been recorded in approximately 70% of the subjects tested within the species exhibiting these emissions, with approximately one to four SOAEs per ear. On average, the frequency spacing between consecutive SOAEs from the same ear is  $\sim 0.5$  octave, exceeding the frequency spacing found in humans ( $\sim 0.1$  octave; reviewed in van Dijk et al. 1989). SOAE spectral peaks are limited within the 450 to 1350 Hz frequency range (van Dijk et al. 1989), suggesting that SOAEs may only arise from the caudal portion of the AP (van Dijk and Manley 2001).

Similar to SFOAEs and AP-DPOAEs, SOAEs are sensitive to changes in temperature. Lowering (increasing) the subjects' body temperature results in lower

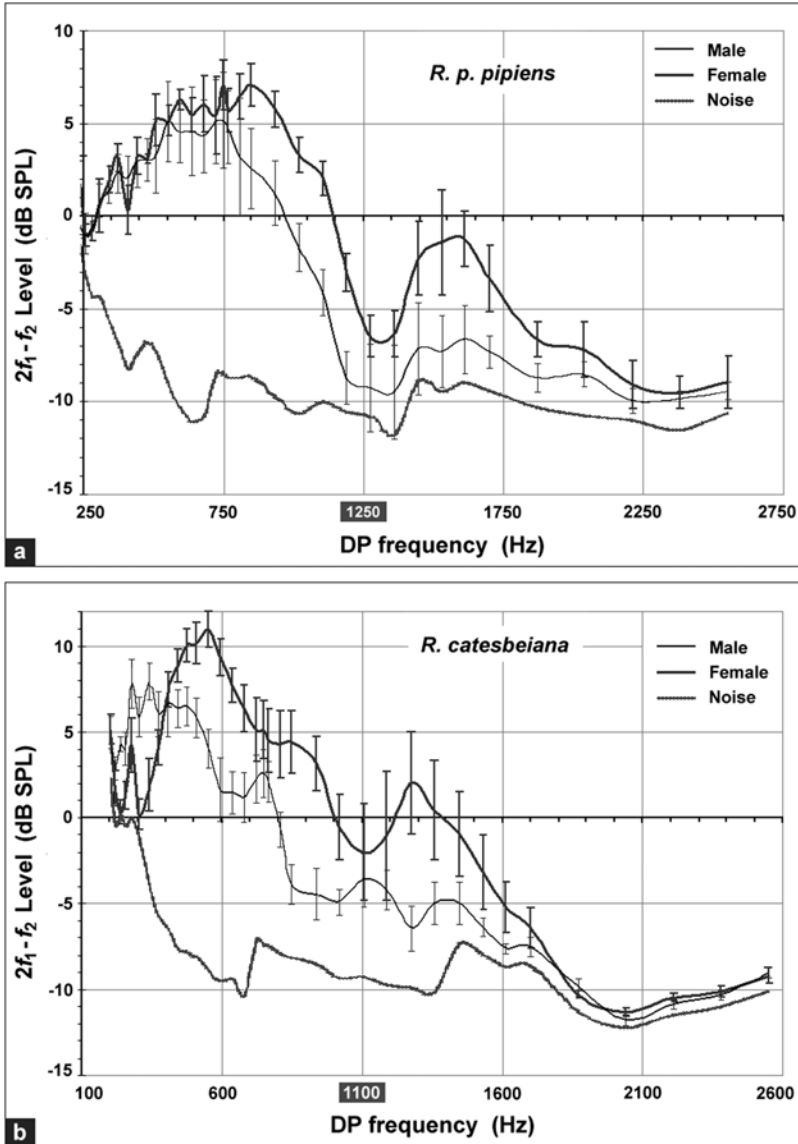


FIGURE 7.11. Comparison between DPOAE ( $2f_1 - f_2$ ) audiograms from both ears of five male and five female *R. p. pipiens* (A) and *R. catesbeiana* (B). DPOAE levels are plotted as a function of DP frequency. Female subjects exhibit stronger emissions than males, especially from the BP (from Vassilakis et al. 2004).

(higher) SOAE frequencies (van Dijk and Wit 1987; van Dijk et al. 1989; Long et al. 1996). The rate of this change appears to depend on emission frequency, with SOAEs <600Hz exhibiting less sensitivity to temperature changes than SOAEs >600Hz (Long et al. 1996; van Dijk et al. 1996; Fig. 7.12). Temperature changes also affect SOAE amplitudes, but in an on-off rather than continuous manner (van Dijk and Wit 1987).

Both the frequency and amplitude of SOAEs change in the presence of an external sinusoidal stimulus. If the external stimulus is both close in frequency to an SOAE and sufficiently strong, the SOAE frequency will shift to match the frequency of the stimulus (van Dijk and Wit 1990). On the contrary, if the frequency separation between an SOAE and the external stimulus is large, the SOAE frequency will shift away from that of the external stimulus (Baker et al. 1989;

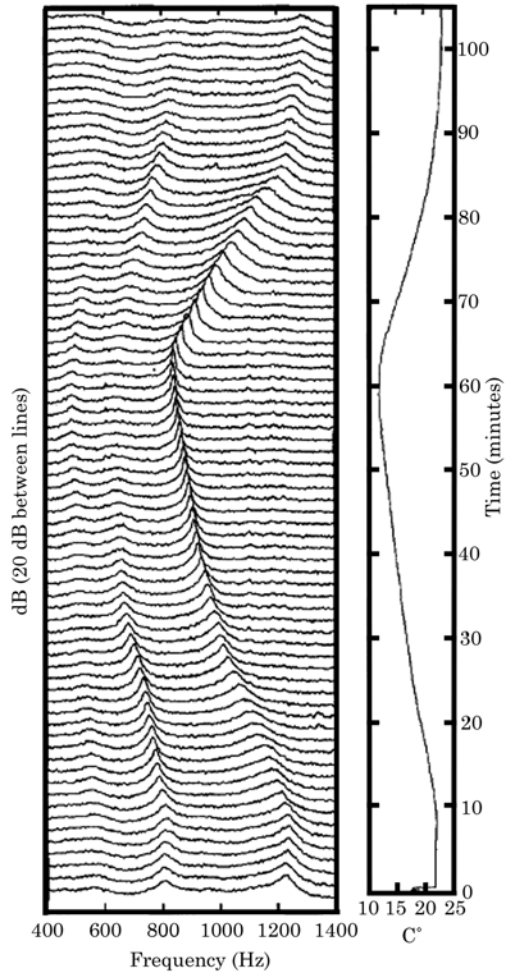


FIGURE 7.12. SOAE spectra (64 averages per spectrum) and temperature changes plotted over time, illustrating the dependence of SOAE frequencies on temperature. From Long et al. (1996).

Long et al. 1996). The presence of an external stimulus may also decrease the amplitude of an SOAE. The amount of suppression depends on the frequency of the external stimulus, as seen in isosuppression contours (Baker et al. 1989). Suppression is most prominent when the SOAE and the external stimulus coincide in frequency, and decreases as the frequency separation between the two increases. The amount of suppression is highest for external stimulus frequencies below the SOAE frequency, resulting in asymmetric isosuppression contours that are similar in shape to neural tuning curves (Baker et al. 1989).

Although SOAEs could be easily recorded in the summer, they were not detected in the winter (van Dijk et al. 1989), confirming the earlier observation that OAE generation may be seasonal.

#### *4.5 OAEs Suggest the BP Acts as a Single Auditory Filter*

Due to the BP's relatively simple anatomy and physiology, it has been suggested that this papilla may be functioning as a bandpass filter with a single CF. In ranid frogs, for example, all BP hair bundles follow the same orientation (Lewis 1978), and almost all BP nerve fibers are tuned to the same frequency and have identically shaped tuning curves (Ronken 1990). Based on such observations, several frog DPOAE studies have used the Duffing oscillator as a model for the BP (van Dijk and Manley 2001; Meenderink et al. 2005a,b), successfully predicting the dependence of DPOAE amplitudes and phases on the relative and absolute primary frequencies, as well as the observed correlations between DPOAEs and neural tuning curves. These results support the notion of the BP as a single, broadly tuned auditory filter. The uniqueness of this property within vertebrate hearing makes the frog an excellent subject for DPOAE studies, inasmuch as BP-DPOAEs are not influenced by auxiliary structures (in contrast to the mammalian ear or the frog AP) and only reflect the properties of the nonlinearities directly involved in OAE generation.

#### *4.6 OAEs and Inner Ear Amplification in the Frog*

OAE data obtained from the frog support several speculations regarding the functioning of the amphibian inner ear. It is generally accepted that mammalian OAE generation is closely linked to the cochlear amplifier, a term introduced by Davis (1983) to denote the summed contribution of those mechanisms that appear to enhance the movement of mammalian inner ear structures. Besides the presence of OAEs, several observations support the involvement of an amplifier in the ear's transduction of sound. First, the auditory system exhibits higher sensitivity and frequency selectivity than expected by its passive mechanical properties alone. Second, the system's response grows compressively, being highly amplified for low-intensity stimuli and less so as stimulus intensity increases. Third, the system is highly susceptible to various forms of physical, physiological, and chemical insults, consistent with the fact that the cochlear amplifier depends on biochemical sources for its energy.

SOAEs are the only type of OAEs whose mere occurrence may be interpreted as evidence for the presence of an inner ear amplifier. In the frog, SOAEs have been measured only within a frequency range corresponding to the frequency response of the AP, suggesting that an amplification process may be present in this papilla but not in the BP. Several differences between AP- and BP-DPOAEs support this observation. Only DPOAE I/O curves from the AP exhibit compressive growth at low primary levels. Furthermore, low-level AP-DPOAEs are much more sensitive to physiological insults and changes in temperature than low-level BP-DPOAEs, suggesting the presence of biochemical energy sources in the AP that would power an amplifier.

An amplification process may therefore be present in the frog AP but not in the BP. This potential difference is consistent with and may be related to several physiological differences between the two papillae. In the *R. catesbeiana* ear, for example, the AP has approximately fifteen times as many hair cells and is innervated by approximately three times as many afferent nerve fibers as the BP (Geisler et al. 1964; Lewis et al. 1985). At the same time, efferent nerve fibers, in most cases, innervate the AP but not the BP (Robbins et al. 1967; Simmons et al. 1995).

It has been suggested that, because the AP is tonotopically organized (Lewis et al. 1982b; Simmons et al. 1992) and the BP responds as a bandpass filter with a single characteristic frequency (van Dijk and Manley 2001), the presence of an amplifier might play the role of increasing the sharpness of tuning of the AP fibers (Vassilakis et al. 2004). The absence of an amplifier from the BP may be beneficial as well. Due to their ectothermic physiology, frog bodies may undergo relatively large temperature fluctuations. Given the lack of temperature sensitivity of the BP fibers (Stiebler and Narins 1990; van Dijk et al. 1990), such fluctuations do not result in the loss of frequency-specific information from this sensory organ.

Although specifying the exact location and the underlying molecular motor of a possible AP amplifier is not essential to understanding whether amplification occurs in the frog ear, some relevant speculations can be made. According to general consensus, the inner ear amplifier is located within the sensory hair cells. In mammals, a likely candidate for the cochlear amplifier has been identified in the OHCs. These cells contain within their lateral membrane a protein (prestin) that undergoes voltage-mediated conformational changes (Santos-Sacchi 1991). This deformation alters the OHC shape in synchrony with an incoming stimulus, providing a cycle-by-cycle amplification of the stimulus-induced OHC movement (Zheng et al. 2000). Nonmammalian vertebrates, on the other hand, lack OHCs and there is no evidence of or likelihood for fast somatic motility of their hair cells (Manley 2001). Oscillation of the hair bundles has been proposed as an alternative amplification mechanism. Such oscillations have been observed *in vitro* in several nonmammalian vestibular organs (Hudspeth 1997) and in the hearing organ of turtles (Crawford and Fettiplace 1985), and *in vivo* in the bobtail lizard (Manley et al. 2001). Great interest has been generated from recent reports (Chan

and Hudspeth 2005; Jia and He 2005) documenting active hair bundle motion in mammalian hair cell bundles, requiring a reassessment of the role of evolution in the genesis of motility in auditory hearing organs.

## 5. Summary

The sensitivity (e.g., spontaneous activity and thresholds) and tuning (e.g., frequency responses) of the frog auditory periphery is determined in large part by its unique anatomical and physiological features, not the least of which is that there are two organs specialized for the reception of airborne sounds. The frog ear relies heavily on an elaborate infrastructure, which subserves conduction, filtering, and transduction of auditory information by both the AP (low to mid-frequencies) and the BP (high frequencies).

As the input to the central auditory system, auditory nerve fiber responses are determined by the arrangement and number of their connections to hair cells, by the events at the hair cell synapse, by the intrinsic properties of hair cells and their hair bundles, as well as by the bandpass spectral filtering of the overlying tectorial structures. The frog AP is a uniquely organized tonotopic end-organ whereas the frog BP is a broadly tuned organ that acts as a single auditory filter. In both the AP and BP, hair cells are rigidly fixed to a cartilaginous wall and lack a basilar membrane, a structure common to auditory organs of reptiles, birds, and mammals. The frog AP has a complicated frequency-related distribution of hair bundle types with polarization patterns that grossly correspond to other rostrocaudal gradients in the ear, such as hair cell height and tectorial membrane mass.

In the frog inner ear, frequency selectivity may depend on the mechanics of the tectorium and the fluids as well as their interaction with the hair cells. Movement of the tectorium presumably produces deflection of the stereovilli that leads to the release of transmitter, activating auditory nerve fibers. Thus, the inertial lag times associated with tectorium mechanics along with differences in stereovillar lengths or stiffness may be the primary determinants of response latency. Determination of the actual travel times of action potentials in auditory nerve fibers from high- and low-frequency locations should give a better understanding of how the motion of the tectorium is coupled to the stereovillar bundle.

Rostrocaudal variations in hair cell height are inversely related to tonotopy such that the tallest hair cells are found in the lowest-frequency regions and shorter hair cells are found in higher-frequency regions. Whole-cell capacitances also covary with hair cell body length. Thus, basic morphological features (e.g., hair cell height) can be related to the presence of intrinsic electrical tuning mechanisms (e.g., capacitance and frequency tuning). The variation of synaptic architecture is consistent with innervation patterns: rostrally located hair cells have a greater number of synapses and nerve fiber contacts than caudally located hair cells. Similarly, efferent synapses are predominant in rostral areas and not detectable in caudal areas. Frog auditory nerve fibers also have anatomical and

physiological gradients such as larger diameters and longer response latencies from low-frequency rostral fibers, and thinner diameters and shorter response latencies from higher-frequency caudal fibers.

It is currently well-established that the mammalian cochlea exhibits tonotopic organization (Von Békésy, 1960). This tonotopy arises from mass and stiffness gradients along the basilar membrane and can be observed by measuring the mechanical response of the basilar membrane (Robles and Ruggero 2001). One of the most intriguing manifestations of this gradient-induced tonotopy is the presence of traveling waves on the basilar membrane. Conversely, tonotopic organization that does not move gradually from low to high frequencies (or vice versa) cannot support a traveling wave. Because the AP is also tonotopically organized, with highest sensitivity to different frequencies distributed at different locations along the sensory epithelium, the question arises whether this papilla may also support traveling waves. Neurophysiological evidence (Hillery and Narins 1984) suggests that this may indeed be the case. However, if there is an absence of appropriate mass and stiffness gradients within the tectorium (or any other frog inner ear structure) then the presence of mammalianlike traveling waves in the AP may be excluded (Lewis et al. 1985). This exclusion is further supported by the patterns present in DPOAE ( $f_1$ ,  $f_2$ ) area maps (Meenderink et al. 2005a). Rather, it seems more plausible that the tectorium overlying the AP sensory epithelium functions as a broadband filter, with tonotopy originating in additional filtering mechanisms (mechanical and/or electrical) that may be closely associated with the hair cells. Data on the dependence of DPOAE amplitude on primary level difference ( $L_1-L_2$ ) also suggest that the tectorium may function as a broadband filter (Vassilakis et al. 2004; Meenderink and van Dijk 2005a), outlining the boundaries of the AP frequency response range. A possible difference in DPOAE generation sites between mammals and frogs observed by Vassilakis et al. (2004) also questions the development of a mammalianlike traveling wave in the frog ear.

OAEs are indirect manifestations of the vibration of structures within the AP and, as such, they can only provide indirect evidence for the types of available spectral filtering (i.e., the presence or absence of traveling waves). Conclusive evidence for the presence of a traveling wave can best be obtained by directly recording the vibration of the tectorial membrane or of other traveling-wave relevant AP structures.

*Acknowledgments.* The authors are indebted to Peter M. Narins for his superb editorship, guidance, and assistance. His gentle spirit, encouraging words, and persistent intellectual rigor were invaluable to the writing of this chapter.

## References

- Abdala C (2000) Distortion product otoacoustic emission (2f1-f2) amplitude growth in human adults and neonates. *J Acoust Soc Am* 107:446-456.

- Ashmore JF, Geleoc GS, Harbott L (2000) Molecular mechanisms of sound amplification in the mammalian cochlea. *Proc Natl Acad Sci USA* 97:11759–11764.
- Baird RA, Burton MD, Fashena DS, Naeger RA (2000) Hair cell recovery in mitotically blocked cultures of the bullfrog saccule. *Proc Natl Acad Sci USA* 97:11722–11729.
- Baird RA, Lewis ER (1986) Correspondences between afferent innervation patterns and response dynamics in the bullfrog utricle and lagena. *Brain Res* 369:48–64.
- Baker RJ, Wilson JP, Whitehead ML (1989) Otoacoustic evidence for nonlinear behavior in frog hearing: suppression but no distortion products. In: Wilson J, Kemp DT (eds.) *Cochlear Mechanisms: Structure, Function and Models*. Plenum, New York, pp. 349–356.
- Benedix JH, Jr., Pedemonte M, Velluti R, Narins PM (1994) Temperature dependence of two-tone rate suppression in the northern leopard frog, *Rana pipiens pipiens*. *J Acoust Soc Am* 96:2738–2745.
- Bleeck S, Langner G (2001) Functional significance of latencies. In: Greenberg S, Slaney M (eds.) *Computational Models of Auditory Function* (NATO Science Series). IOS Press, Burke, VA, pp. 205–220.
- Bozovic D, Hudspeth AJ (2003) Hair-bundle movements elicited by transepithelial electrical stimulation of hair cells in the sacculus of the bullfrog. *Proc Natl Acad Sci USA* 100:958–963.
- Capranica RR (1978) Auditory processing in anurans. *Fed Proc* 37:2324–2328.
- Capranica RR, Moffat AJM (1975) Selectivity of the peripheral auditory system of spadefoot toads (*Scaphiopus couchi*) for sounds of biological significance. *J Comp Physiol* 100.
- Capranica RR, Moffat AJM (1980) Nonlinear properties of the peripheral auditory system of anurans. In: Popper AN, Fay RR (eds.) *Comparative Studies of Hearing in Vertebrates*. Springer, New York, pp. 139–165.
- Capranica RR, Moffat AJM (1983) Neurobehavioral correlates of sound communication in anurans. In: Ewert J, Capranica R, Ingle D (eds.) *Advances in Vertebrate Neuroethology*. Plenum, New York, pp. 701–730.
- Carey MB, Zelick R (1993) The effect of sound level, temperature and dehydration on the brainstem auditory evoked potential in anuran amphibians. *Hear Res* 70:216–228.
- Chan DK, Hudspeth AJ (2005) Ca<sup>2+</sup> current-driven nonlinear amplification by the mammalian cochlea in vitro. *Nat Neurosci* 8:149–155.
- Chang JS, Popper AN, Saidel WM (1992) Heterogeneity of sensory hair cells in a fish ear. *J Comp Neurol* 324:621–640.
- Christensen-Dalsgaard J, Jørgensen MB (1996) One-tone suppression in the frog auditory nerve. *J Acoust Soc Am* 100:451–457.
- Christensen-Dalsgaard J, Jørgensen MB, Kannevorff M (1998) Basic response characteristics of auditory nerve fibers in the grassfrog (*Rana temporaria*). *Hear Res* 119:155–163.
- Corwin JT, Warchol ME (1991) Auditory hair cells: Structure, function, development, and regeneration. *Ann Rev Neurosci* 14:301–333.
- Crawford AC, Fettiplace R (1985) The mechanical properties of ciliary bundles of turtle cochlear hair cells. *J Physiol* 364:359–379.
- Dallos P (1992) The active cochlea. *J Neurosci* 12:4575–4585.
- Davis H (1983) An active process in cochlear mechanics. *Hear Res* 9:79–90.
- De Boer E (1967) Correlation studies applied to the frequency resolution of the cochlea. *J Aud Res* 7:209–217.

- Deutsch S (1969) The maximization of nerve conduction velocity. *IEEE Trans Syst Sci Cybern* 5:86–91.
- Dunia R, Narins PM (1989) Temporal resolution in frog auditory-nerve fibers. *J Acoust Soc Am* 85:1630–1638.
- Eggermont JJ (1993) Wiener and Volterra analyses applied to the auditory system. *Hear Res* 66:177–201.
- Ehret G, Moffat AJM, Capranica RR (1983) Two-tone suppression in auditory nerve fibers of the green treefrog (*Hyla cinerea*). *J Acoust Soc Am* 73:2093–2095.
- Emmerich E, Richter F, Reinhold U, Linss V, Linss W (2000) Effects of industrial noise exposure on distortion product otoacoustic emissions (DPOAEs) and hair cell loss of the cochlea—long term experiments in awake guinea pigs. *Hear Res* 148:9–17.
- Faulstich M, Kössl M (2000) Evidence for multiple DPOAE components based upon group delay of the 2f(1)-f(2) distortion in the gerbil. *Hear Res* 140:99–110.
- Feng AS, Narins PM, Capranica RR (1975) Three populations of primary auditory fibers in the bullfrog (*Rana catesbeiana*): Their peripheral origins and frequency sensitivities. *J Comp Physiol* 100:221–229.
- Feng AS, Shofner WP (1981) Peripheral basis of sound localization in anurans. Acoustic properties of the frog's ear. *Hear Res* 5:201–216.
- Fettiplace R, Ricci AJ, Hackney CM (2001) Clues to the cochlear amplifier from the turtle ear. *Trends Neurosci* 24:169–175.
- Fitzgerald JV, Burkitt AN, Clark GM, Paolini AG (2001) Delay analysis in the auditory brainstem of the rat: Comparison with click latency. *Hear Res* 159:85–100.
- Flock A (1965) Transducing mechanisms in the lateral line canal organ receptors. *Cold Spring Harb Symp Quant Biol* 30:133–145.
- Flock A, Flock B (1966) Ultrastructure of the amphibian papilla in the bullfrog. *J Acoust Soc Am* 40:1262.
- Frishkopf LS, Flock A (1974) Ultrastructure of the basilar papilla, an auditory organ in the bullfrog. *Acta Otolaryngol* 77:176–184.
- Geisler CD, Van Bergeijk W, Frishkopf LS (1964) The inner ear of the bullfrog. *J Morphol* 114:43–57.
- Gleich O, Wilson S (1993) The diameters of guinea pig auditory nerve fibres: Distribution and correlation with spontaneous rate. *Hear Res* 71:69–79.
- Gleisner L, Flock A, Wersall J (1973) The ultrastructure of the afferent synapse on hair cells in the frog labyrinth. *Acta Otolaryngol* 76:199–207.
- Gold T (1948) Hearing. II. The physical basis of the action of the cochlea. *Proc Roy Soc London B, Biological Sciences* 135:492–498.
- Hau LWT, Simmons DD, Narins PM (2004) Frequency-dependence of auditory-nerve latency in the northern leopard frog, *Rana pipiens pipiens*. *Assoc for Research in Otolaryngology Abstract* 380.
- Hetherington TE, Jaslow AP, Lombard RE (1986) Comparative morphology of the amphibian opercularis system: I. General design features and functional interpretation. *J Morphol* 190:43–61.
- Hillery CM, Narins PM (1984) Neurophysiological evidence for a traveling wave in the amphibian inner ear. *Science* 225:1037–1039.
- Hillery CM, Narins PM (1987) Frequency and time domain comparison of low-frequency auditory fiber responses in two anuran amphibians. *Hear Res* 25:233–248.
- Hödl W, Amezcua A, Narins PM (2004) The role of call frequency and the auditory papillae in phonotactic behavior in male dart-poison frogs *Epipedobates femoralis* (Dendrobatidae). *J Comp Physiol A* 190:823–829.

- Hudspeth AJ (1997) How hearing happens. *Neuron* 19:947–950.
- Hudspeth AJ, Corey DP (1977) Sensitivity, polarity, and conductance change in the response of vertebrate hair cells to controlled mechanical stimuli. *Proc Natl Acad Sci USA* 74:2407–2411.
- Hudspeth AJ, Choe Y, Mehta AD, Martin P (2000) Putting ion channels to work: mechano-electrical transduction, adaptation, and amplification by hair cells. *Proc Natl Acad Sci USA* 97:11765–11772.
- Jia S, He DZ (2005) Motility-associated hair-bundle motion in mammalian outer hair cells. *Nat Neurosci* 8:1028–1034.
- Kalluri R, Shera CA (2001) Distortion-product source unmixing: A test of the two-mechanism model for DPOAE generation. *J Acoust Soc Am* 109:622–637.
- Kemp DT (1978) Stimulated acoustic emissions from within the human auditory system. *J Acoust Soc Am* 64:1386–1391.
- Kiang NYS, Watanabe T, Thomas L, Clark L (1965) *Discharge Patterns of Single Fibers in the Cat's Auditory Nerve*. MIT Press, Cambridge, MA.
- Knight RD, Kemp DT (2000) Indications of different distortion product otoacoustic emission mechanisms from a detailed f1, f2 area study. *J Acoust Soc Am* 107:457–473.
- Knight RD, Kemp DT (2001) Wave and place fixed DPOAE maps of the human ear. *J Acoust Soc Am* 109:1513–1525.
- Köppl C (1995) Otoacoustic emissions as an indicator for active cochlear mechanics: a primitive property of vertebrate auditory organs. In: Manley GA, Klump GM, Köppl C, Fastl H, Oeckinghaus H (eds.), *Advances in Hearing Research*, World Scientific, Singapore, pp. 207–216.
- Köppl C, Authier S (1995) Quantitative anatomical basis for a model of micromechanical frequency tuning in the Tokay gecko, *Gekko gekko*. *Hear Res* 82:14–25.
- Kössl M, Boyan G (1998) Acoustic distortion products from the ear of a grasshopper. *J Acoust Soc Am* 104:326–335.
- Kössl M, Vater M (1996) Further studies on the mechanics of the cochlear partition in the mustached bat. II. A second cochlear frequency map derived from acoustic distortion products. *Hear Res* 94:78–86.
- Kummer P, Janssen T, Hulin P, Arnold W (2000) Optimal L(1)–L(2) primary tone level separation remains independent of test frequency in humans. *Hear Res* 146:47–56.
- Lenzi D, Runyeon JW, Crum J, Ellisman MH, Roberts WM (1999) Synaptic vesicle populations in saccular hair cells reconstructed by electron tomography. *J Neurosci* 19:119–132.
- Lewis ER (1976) Surface morphology of the bullfrog amphibian papilla. *Brain Behav Evol* 13:196–215.
- Lewis ER (1978) Comparative studies of the anuran auditory papillae. *Scan Electron Microsc* 11:633–642.
- Lewis ER (1981) Suggested evolution of tonotopic organization in the frog amphibian papilla. *Neurosci Lett* 21:131–136.
- Lewis ER (1984) On the frog amphibian papilla. *Scan Electron Microsc Pt 4*:1899–1913.
- Lewis ER (1988) Tuning in the bullfrog ear. *Biophys J* 53:441–447.
- Lewis ER, Leverenz EL (1983) Morphological basis for tonotopy in the anuran amphibian papilla. *Scan Electron Microsc Pt 1*:189–200.
- Lewis ER, Li CW (1975) Hair cell types and distributions in the otolithic and auditory organs of the bullfrog. *Brain Res* 83:35–50.

- Lewis ER, Lombard R (1988) The amphibian inner ear. In: Fritzsche B, Ryan M, Wilczynski W, Hetherington T, Walkowiak W (eds.) *The Evolution of the Amphibian Auditory System*. Wiley Interscience, New York, pp. 93–124.
- Lewis ER, Narins PM (1999) The acoustic periphery of amphibians: Anatomy and physiology. In: Fay R, Popper A (eds.) *Comparative Hearing: Fish and Amphibians*. Springer, New York, pp. 101–154.
- Lewis ER, van Dijk P (2004) New variation on the derivation of spectro-temporal receptive fields for primary auditory afferent axons. *Hear Res* 189:120–136.
- Lewis ER, Baird RA, Leverenz EL, Koyama H (1982a) Inner ear: Dye injection reveals peripheral origins of specific sensitivities. *Science* 215:1641–1643.
- Lewis ER, Hecht EI, Narins PM (1992) Diversity of form in the amphibian papilla of Puerto Rican frogs. *J Comp Physiol [A]* 171:421–435.
- Lewis ER, Henry KR, Yamada WM (2002) Tuning and timing of excitation and inhibition in primary auditory nerve fibers. *Hear Res* 171:13–31.
- Lewis ER, Leverenz EL, Bialek WS (1985) *The Vertebrate Inner Ear*. CRC, Boca Raton, FL.
- Lewis ER, Leverenz EL, Koyama H (1982b) The tonotopic organization of the bullfrog amphibian papilla, an auditory organ lacking a basilar membrane. *J Comp Physiol* 145:437–445.
- Liberman MC (1980) Morphological differences among radial afferent fibers in the cat cochlea: an electron-microscopic study of serial sections. *Hear Res* 3:45–63.
- Liberman MC, Simmons DD (1985) Applications of neuronal labeling techniques to the study of the peripheral auditory system. *J Acoust Soc Am* 78:312–319.
- Liberman MC, Dodds LW, Pierce S (1990) Afferent and efferent innervation of the cat cochlea: Quantitative analysis with light and electron microscopy. *J Comp Neurol* 301:443–460.
- Liberman MC, Gao J, He DZ, Wu X, Jia S, Zuo J (2002) Prestin is required for electromotility of the outer hair cell and for the cochlear amplifier. *Nature* 419:300–304.
- Liff HJ, Goldstein MH, Jr. (1970) Peripheral inhibition in auditory fibers in the frog. *J Acoust Soc Am* 47:1538–1547.
- Lnenicka GA, Atwood HL, Marin L (1986) Morphological transformation of synaptic terminals of a phasic motoneuron by long-term tonic stimulation. *J Neurosci* 6:2252–2258.
- Long GR, van Dijk P, Wit HP (1996) Temperature dependence of spontaneous otoacoustic emissions in the edible frog (*Rana esculenta*). *Hear Res* 98:22–28.
- Lonsbury-Martin BL, McCoy MJ, Whitehead ML, Martin GK (1993) Clinical testing of distortion-product otoacoustic emissions. *Ear Hear* 14:11–22.
- Maison S, Micheyl C, Collet L (1997) Medial olivocochlear efferent system in humans studied with amplitude-modulated tones. *J Neurophysiol* 77:1759–1768.
- Manley GA (2001) Evidence for an active process and a cochlear amplifier in nonmammals. *J Neurophysiol* 86:541–549.
- Manley GA, Kirk DL, Koppl C, Yates GK (2001) In vivo evidence for a cochlear amplifier in the hair-cell bundle of lizards. *Proc Natl Acad Sci USA* 98:2826–2831.
- Mason MJ, Lin CC, Narins PM (2003) Sex differences in the middle ear of the bullfrog (*Rana catesbeiana*). *Brain Behav Evol* 61:91–101.
- Meenderink SWF, van Dijk P (2004) Level dependence of distortion product otoacoustic emissions in the leopard frog, *Rana pipiens pipiens*. *Hear Res* 192:107–118.
- Meenderink SWF, van Dijk P (2005a) Characteristics of distortion product otoacoustic emissions in the frog from L1, L2 maps. *J Acoust Soc Am* 118:279–286.

- Meenderink SWF, van Dijk P (2005b) Temperature dependence of distortion product otoacoustic emissions in the frog. *in preparation*.
- Meenderink SWF, Narins PM, van Dijk P (2005a) Detailed f1, f2 area study of distortion product otoacoustic emissions in the frog. *J Assoc Res Otolaryngol* 6:37–47.
- Meenderink SWF, van Dijk P, Narins PM (2005b) Comparison between distortion product otoacoustic emissions and nerve fiber responses from the basilar papilla of the frog. *J Acoust Soc Am* 117:3165–3173.
- Mills DM, Rubel EW (1994) Variation of distortion product otoacoustic emissions with furosemide injection. *Hear Res* 77:183–199.
- Narins PM (1983) Synchronous vocal response mediated by the amphibian papilla in a neotropical treefrog: Behavioral evidence. *J Exp Biol* 105:95–105.
- Narins PM, Capranica RR (1976) Sexual differences in the auditory system of the treefrog, *Eleutherodactylus coqui*. *Science* 192:378–380.
- Nobili R, Mammano F, Ashmore J (1998) How well do we understand the cochlea? *Trends Neurosci* 21:159–167.
- Owens JJ, McCoy MJ, Lonsbury-Martin BL, Martin GK (1992) Influence of otitis media on evoked otoacoustic emission in children. *Seminars in Hearing* 13:53–65.
- Owens JJ, McCoy MJ, Lonsbury-Martin BL, Martin GK (1993) Otoacoustic emissions in children with normal ears, middle ear dysfunction, and ventilating tubes. *Am J Otol* 14:34–40.
- Palmer AR, Wilson JP (1982) Spontaneous and evoked acoustic emissions in the frog *Rana esculenta*. *J Physiol* 324:66.
- Pitchford S, Ashmore JF (1987) An electrical resonance in hair cells of the amphibian papilla of the frog *Rana temporaria*. *Hear Res* 27:75–83.
- Probst R, Lonsbury-Martin BL, Martin GK (1991) A review of otoacoustic emissions. *J Acoust Soc Am* 89:2027–2067.
- Purgue AP, Narins PM (2000a) Mechanics of the inner ear of the bullfrog (*Rana catesbeiana*): The contact membranes and the periotic canal. *J Comp Physiol [A]* 186:481–488.
- Purgue AP, Narins PM (2000b) A model for energy flow in the inner ear of the bullfrog (*Rana catesbeiana*). *J Comp Physiol [A]* 186:489–495.
- Robbins RG, Bauknight RS, Honrubia V (1967) Anatomical distribution of efferent fibers in the 8th cranial nerve of the bullfrog (*Rana catesbeiana*). *Acta Otolaryngol* 64:436–448.
- Robles L, Ruggero MA (2001) Mechanics of the mammalian cochlea. *Physiol Rev* 81:1305–1352.
- Ronken DA (1990) Basic properties of auditory-nerve responses from a “simple” ear: The basilar papilla of the frog. *Hear Res* 47:63–82.
- Ronken DA (1991) Spike discharge properties that are related to the characteristic frequency of single units in the frog auditory nerve. *J Acoust Soc Am* 90:2428–2440.
- Ronken DA, Bosch WR, Molnar CE (1993) Effects of spike discharge history on discharge probability and latency in frog basilar papilla units. *Hear Res* 69:55–75.
- Rose GJ, Capranica RR (1985) Sensitivity to amplitude modulated sounds in the anuran auditory nervous system. *J Neurophysiol* 53:446–465.
- Rosowski JJ, Peake WT, White JR (1984) Cochlear nonlinearities inferred from two-tone distortion products in the ear canal of the alligator lizard. *Hear Res* 13:141–158.
- Rushton WA (1951) A theory of the effects of fibre size in medullated nerve. *J Physiol* 115:101–122.

- Santos-Sacchi J (1991) Reversible inhibition of voltage-dependent outer hair cell motility and capacitance. *J Neurosci* 11:3096–3110.
- Schetzen M (1989) *The Volterra and Wiener Theories of Nonlinear Systems*. Krieger, Malabar, FL.
- Schneider S, Prijs VF, Schoonhoven R (2003) Amplitude and phase of distortion product otoacoustic emissions in the guinea pig in an (f1,f2) area study. *J Acoust Soc Am* 113:3285–3296.
- Shera CA, Guinan JJ, Jr. (1999) Evoked otoacoustic emissions arise by two fundamentally different mechanisms: A taxonomy for mammalian OAEs. *J Acoust Soc Am* 105:782–798.
- Shofner WP, Feng AS (1983) A quantitative light microscopic study of the bullfrog amphibian papilla tectorium: Correlation with the tonotopic organization. *Hear Res* 11:103–116.
- Shofner WP, Feng AS (1984) Quantitative light and scanning electron microscopic study of the developing auditory organs in the bullfrog: Implications on their functional characteristics. *J Comp Neurol* 224:141–154.
- Simmons AM (1988) Masking patterns in the bullfrog (*Rana catesbeiana*). I: Behavioral effects. *J Acoust Soc Am* 83:1087–1092.
- Simmons AM, Reese G, Ferragamo M (1993) Periodicity extraction in the anuran auditory nerve. II: Phase and temporal fine structure. *J Acoust Soc Am* 93:3374–3389.
- Simmons DD, Narins PM (1995) Conduction velocity, fiber diameter and response latency in auditory nerve fibers of *Rana pipiens pipiens*: Toward temporal separation of coincidence? *Proceedings of the 4th International Congress of Neuroethology*. 347.
- Simmons DD, Bertolotto C, Leong M (1994a) Ultrastructural reconstruction of auditory hair cells and their synapses in low and high frequency regions of the frog inner ear. *Proc Int'l Cong Electr Micrs* 13:629–630.
- Simmons DD, Bertolotto C, Narins PM (1994b) Morphological gradients in sensory hair cells of the amphibian papilla of the frog, *Rana pipiens pipiens*. *Hear Res* 80:71–78.
- Simmons DD, Bertolotto C, Leong M (1995) Synaptic ultrastructure within the amphibian papilla of *Rana pipiens pipiens*: rostrocaudal differences. *Auditory Neurosci* 1:183–193.
- Simmons DD, Bertolotto C, Narins PM (1992) Innervation of the amphibian and basilar papillae in the leopard frog: Reconstructions of single labeled fibers. *J Comp Neurol* 322:191–200.
- Simmons DD, Burton MD, Hooper RN, Baird RA (2004) Hair cell damage and recovery from high-level noise exposures in the amphibian papilla of the bullfrog. Association for Research in Otolaryngology Abstract #365.
- Smith CA, Sjostrand FS (1961) Structure of the nerve endings on the external hair cells of the guinea pig cochlea as studied by serial section. *J Ultrastruc Res* 5:184–192.
- Smith RS, Koles ZJ (1970) Myelinated nerve fibers: Computed effect of myelin thickness on conduction velocity. *Am J Physiol* 219:1256–1258.
- Smotherman MS, Narins PM (1999a) The electrical properties of auditory hair cells in the frog amphibian papilla. *J Neurosci* 19:5275–5292.
- Smotherman MS, Narins PM (1999b) Potassium currents in auditory hair cells of the frog basilar papilla. *Hear Res* 132:117–130.
- Smotherman MS, Narins PM (2000) Hair cells, hearing and hopping: A field guide to hair cell physiology in the frog. *J Exp Biol* 203:2237–2246.
- Sobkowicz HM, Rose JE, Scott GL, Levenick CV (1986) Distribution of synaptic ribbons in the developing organ of Corti. *J Neurocytol* 15:693–714.

- Stiebler IB, Narins PM (1990) Temperature-dependence of auditory nerve response properties in the frog. *Hear Res* 46:63–81.
- Stover L, Gorga MP, Neely ST, Montoya D (1996) Toward optimizing the clinical utility of distortion product otoacoustic emission measurements. *J Acoust Soc Am* 100: 956–967.
- Sugihara I, Furukawa T (1989) Morphological and functional aspects of two different types of hair cells in the goldfish sacculus. *J Neurophysiol* 62:1330–1343.
- van Dijk P (1995) Polynomial correlation used to estimate the degree of nonlinearity of the frog inner ear system. *J Acoust Soc Am* 97:3414.
- van Dijk P, Manley GA (2001) Distortion product otoacoustic emissions in the tree frog *Hyla cinerea*. *Hear Res* 153:14–22.
- van Dijk P, Wit HP (1987) Temperature dependence of frog spontaneous otoacoustic emissions. *J Acoust Soc Am* 82:2147–2150.
- van Dijk P, Wit HP (1990) Synchronization of spontaneous otoacoustic emissions to a 2f<sub>1</sub>-f<sub>2</sub> distortion product. *J Acoust Soc Am* 88:850–856.
- van Dijk P, Wit HP, Segenhout JM (1989) Spontaneous otoacoustic emissions in the European edible frog (*Rana esculenta*): Spectral details and temperature dependence. *Hear Res* 42:273–282.
- van Dijk P, Lewis ER, Wit HP (1990) Temperature effects on auditory nerve fiber response in the American bullfrog. *Hear Res* 44:231–240.
- van Dijk P, Mason MJ, Narins PM (2002) Distortion product otoacoustic emissions in frogs: correlation with middle and inner ear properties. *Hear Res* 173:100–108.
- van Dijk P, Narins PM, Mason MJ (2003) Physiological vulnerability of distortion product otoacoustic emissions from the amphibian ear. *J Acoust Soc Am* 114:2044–2048.
- van Dijk P, Narins PM, Wang J (1996) Spontaneous otoacoustic emissions in seven frog species. *Hear Res* 101:102–112.
- van Dijk P, Wit HP, Segenhout JM (1997) Dissecting the frog inner ear with Gaussian noise. II. Temperature dependence of inner ear function. *Hear Res* 114:243–251.
- van Dijk P, Wit HP, Segenhout JM, Tubis A (1994) Wiener kernel analysis of inner ear function in the American bullfrog. *J Acoust Soc Am* 95:904–919.
- Vassilakis PN, Meenderink SWF, Narins PM (2004) Distortion product otoacoustic emissions provide clues to hearing mechanisms in the frog ear. *J Acoust Soc Am* 116:3713–3726.
- Von Békésy G (1960) *Experiments in Hearing*. Acoustical Society of America Press, New York.
- Walrond JP, Reese TS (1985) Structure of axon terminals and active zones at synapses on lizard twitch and tonic muscle fibers. *J Neurosci* 5:1118–1131.
- West CD (1985) The relationship of the spiral turns of the cochlea and the length of the basilar membrane to the range of audible frequencies in ground dwelling mammals. *J Acoust Soc Am* 77:1091–1101.
- Wever EG (1973) The ear and hearing in the frog, *Rana pipiens*. *J Morphol* 141:461–477.
- Wever EG (1985) *The Amphibian Ear*. Princeton University, Princeton, NJ.
- Whitehead ML, Lonsbury-Martin BL, Martin GK (1992) Evidence for two discrete sources of 2f<sub>1</sub>-f<sub>2</sub> distortion-product otoacoustic emission in rabbit. II: Differential physiological vulnerability. *J Acoust Soc Am* 92:2662–2682.
- Whitehead ML, Wilson JP, Baker RJ (1986) The effects of temperature on otoacoustic emission tuning properties. In: Moore B, Patterson R (eds.) *Auditory Frequency Selectivity*. Plenum, New York, pp. 39–48.

- Wilczynski W, Keddy-Hector AC, Ryan MJ (1992) Call patterns and basilar papilla tuning in cricket frogs. I. Differences among populations and between sexes. *Brain Behav Evol* 39:229–237.
- Wilczynski W, McClelland BE, Rand AS (1993) Acoustic, auditory, and morphological divergence in three species of neotropical frog. *J Comp Physiol* 172:425–438.
- Will U, Fritzsche B (1988) The eighth nerve of amphibians. In: Fritzsche B, Ryan M, Walczynski W, Hetherington T, Walkowiak W (eds.) *The Evolution of the Amphibian Auditory System*. Wiley-Interscience, New York, pp. 159–183.
- Zakon HH, Capranica RR (1981) An anatomical and physiological study of regeneration of the eighth nerve in the leopard frog. *Brain Res* 209:325–338.
- Zakon HH, Wilczynski W (1988) The physiology of the anuran eighth nerve. In: Fritzsche B, Ryan M, Walczynski W, Hetherington T, Walkowiak W (eds.) *The Evolution of the Amphibian Auditory System*. Wiley-Interscience, New York, pp. 125–155.
- Zelick R, Narins PM (1985) Temporary threshold shift, adaptation, and recovery characteristics of frog auditory nerve fibers. *Hear Res* 17:161–176.
- Zenisek D, Davila V, Wan L, Almers W (2003) Imaging calcium entry sites and ribbon structures in two presynaptic cells. *J Neurosci* 23:2538–2548.
- Zhang M, Abbas PJ (1997) Effects of middle ear pressure on otoacoustic emission measures. *J Acoust Soc Am* 102:1032–1037.
- Zheng J, Shen W, He DZ, Long KB, Madison LD, Dallos P (2000) Prestin is the motor protein of cochlear outer hair cells. *Nature* 405:149–155.